polymer review

Relaxation processes in crystalline polymers: experimental behaviour – a review

Richard H. Boyd
Department of Materials Science and Engineering and Department of Chemical Engineering, University of Utah, Salt Lake City, Utah, 84112, USA
(Received 13 January 1984; revised 23 February 1984)

A comprehensive review of relaxation processes in semi-crystalline polymers is presented. Methods for assignment of phase origin of relaxations are discussed. Experimental results for a variety of polymers ranging from inherently difficulty crystallizable to easily crystallizable are reviewed with emphasis placed on phase origin, phase properties and the effects of the interactions between the crystal and amorphous phases.

(Keywords: semi-crystalline polymers; amorphous fraction; morphological assignment; mechanical relaxation; dielectric relaxation; nuclear magnetic resonance)

INTRODUCTION

The study of relaxation processes in crystalline polymers is a subject of continuing great scientific and technological interest. The practical importance of the subject is evident from the observation that the stiffness of typical crystalline engineering thermoplastics at room temperature is $\frac{1}{3}$–$\frac{1}{5}$ that of the same material at low temperature and that the stiffness can vary with temperature by more than a factor of 10 between low temperature and temperatures of common use. The drop in stiffness or modulus takes place in certain regions of temperature, each associated with an anelastic relaxtion process. In turn these are due to the onset of various types of molecular motions (McCrum *et al.*[1]. A great number of investigations have been undertaken with the purpose of characterizing the relaxations in these materials and there has been great scientific interest in the elucidation and detailed description of the molecular processes underlying them. It is true that progress in the area of molecular interpretation has been slow and there there are often apparently conflicting interpretations of the same processes. It is also true that in the past few years there have been quite a number of developments that when taken in relation to each other do in fact materially clarify the nature of many of the relaxation phenomena. However, because of the large undigested literature many of these developments seem not to be generally appreciated. The present review is an attempt to bring the experimental facts together in a coherent way. This will require sifting through a large number of results, some of them quite recent, some of them not so new. Only with this experimental basis established can the molecular interpretation of relaxation be sensibly addressed. The progress with respect to the latter task will be considered in a separate review.

As a start it is useful to give a capsule version of the relaxation behaviour. In isochronal experiments in the temperature interval between the melting point and liquid nitrogen temperature (−196°C) at least two and often three processes are commonly observed, each with distinct characteristics (see *Table 1* for labelling). In the polymers that show all three, the high temperature α process is commonly considered to be connected with the crystal fraction in the semicrystalline material. The β process in such polymers has been connected with the amorphous fraction and has been associated with the glass–rubber relaxation. In polymers that do not show an α process of the above type the association of the highest temperature process with the glass transition is particularly obvious. The notation α_a is used in discussing this process and its conceptual connection with the β process in polymers possessing a crystalline α process is indicated in *Table 1*. The low temperature process γ (or β where α is missing) is generally agreed to have at least in part amorphous phase origin, but many have considered it to have an important component from the crystal phase also.

It is profitable to further distinguish between certain broad, overlapping yet useful categories of polymers according to their crystallization behaviour. First, polymers with very slow crystallization rates that may be quenched to below the maximum in the crystallization rate vs. undercooling curve, obtained in nearly if not completely amorphous form and conversely are difficult to crystallize to extents of crystallization beyond ~50% will be called inherently 'low' crystallinity polymers. Isotactic polystyrene, aromatic polyesters (e.g. polyethylene terephthalate 'PET') and aromatic polycarbonates (e.g. poly(4-4′-dioxydiphenyl-2,2′propane carbonate 'polycarbonate') are good examples. Second are 'medium' crystallinity polymers that are not ordinarily quenchable to the completely amorphous state, crystallize to extents of crystallinity of 30–60% but are difficult to crystallize to higher extents. Examples are aliphatic polyamides and polyesters. A third category are 'high' crystallinity, rapidly crystallizing polymers that are quenchable in bulk specimens with difficulty down to

Table 1 Notational correspondence

Number of Processes	T_{max} (isochronal) →		
3	γ	β	α
2	β	α_a	–

0032-3861/85/030323-25$03.00

~50% and are ordinarily in the range of 60–80% crystallinity. Examples are linear polyethylene (lPE), polyoxymethylene (POM), polyoxyethylene (POE) and isotactic polypropylene (iPP). Finally it is useful to distinguish a class represented by a copolymer with composition predominately of a monomer whose homopolymer is of the easily crystallizable, high crystallinity type but whose extent of crystallinity is limited by copolymerization. Copolymers of ethylene with propylene or vinyl acetate would be examples. In addition, branched polyethylene (bPE), partially chlorinated polyethylene, and partially hydrogenated polybutadiene and pentenamer, although not prepared by copolymerization, belong to this class.

There are some useful generalizations that can be made about the relaxation behaviour of the above types. The inherently low crystallinity polymers show no crystalline high temperature process but do possess a well-developed amorphous fraction glass–rubber relaxation (α_a). The inherently easily crystallizable, high crystallinity polymers show both α and β relaxations. However, the β process tends to be less prominent than the α_a relaxation in the less easily crystallizable polymers. All of the above types show the low temperature γ (or β when α is missing) process.

Efforts will be made here to carefully document the phase origin of each relaxation and, when this is established, to examine the effect of the relaxation being in a phase intimately connected to another one rather than in a free amorphous or crystalline phase. This interconnection of phases has profound and interesting effects on the relaxation behaviour. The β (or α_a) glass–rubber relaxation is immensely broadened in semi-crystalline specimens. The molecular motions in the crystal responsible for the α process give rise directly to dielectric and n.m.r. relaxation. However, their effect is transferred to the amorphous fraction for mechanical response. In the important case of PE, the γ relaxation can now be definitively assigned entirely to the amorphous state. Subglass γ (or β) relaxations tend to be insensitive to the interconnection of the amorphous fraction (where they reside) to the crystals.

A word about the types of data to be stressed is appropriate. As suggested, these will include mechanical, dielectric and n.m.r. results. The multiple relaxation processes because of their inherent broadness tend to be poorly resolved from each other. The point-by-point temperature scan method is usually resorted to, in trying to resolve them. There is an advantage to dynamic measurements in this respect. For example, dynamic shear modulus G^* gives both an 'integral'-like G' (relaxing between limits) and a 'derivative'-like G'' (with a maximum). The latter materially aids resolution and both together give substantially more information than either alone. Dielectric measurements usually belong to this type. N.m.r. results usually have been of second moments from broad line measurements or relaxation times from various pulse techniques. These results are of the 'integral' type with respect to resolution. Thermal expansion and heat capacity have also been used to study relaxations. The former is of the 'integral' type and the latter tends to be.

MORPHOLOGICAL ASSIGNMENT

Mechanical peak heights and phase assignment

The most obvious and commonly used method for morphological assignment consists of determining what happens to the relaxation strength as the relative amounts of the two phases are varied (through, for example, quenching vs. crystallizing slowly at low degrees of undercooling). At this point, especially in the mechanical case, problems arise. Very often, because they are easily quantified, loss peak heights are used as a measure of relaxation strength (the latter being defined as the difference in limiting values of the property relaxing, i.e. unrelaxed modulus minus relaxed modulus or relaxed dielectric constant minus unrelaxed). A plot of G''_{max}, for instance, is made vs. the (volume) fraction crystallinity. Assuming for the moment that peak heights are a legitimate measure of relaxation strength for the bulk specimen, the fundamental question of course is the following. Does an increase in specimen loss with increasing amorphous content (decreasing crystallinity) imply that the specimen loss has its origin in the amorphous fraction? The question is further complicated by the fact that the same experimental results can be expressed as modulus G^* (G',G'') or compliance J^* (J',J'') or tan $\delta = G''/G' = J''/J'$. Do G''_{max}, J''_{max} and tan δ_{max} plotted against crystallinity all lead to the same conclusion and, if not, which are we to use? The answer is, they do not all necessarily vary in the same direction. To see which should be plotted requires some thought. The main problem is that the recipe for combining the phase moduli to construct the specimen modulus may not be known. Various combining rules have been proposed[2-4], composite theories have been applied[5-9] and certain limiting behaviour or bounds can be established[10,11]. For present purposes, the detailed behaviour need not be known and the following simple phenomenological approach will suffice to answer the question. An upper bound to the modulus of a mixture of isotropic phases is the Voigt, parallel element, uniform strain equation[10],

$$G(\text{upper}) = V_1 G_1 + V_2 G_2 \qquad (1)$$

and a lower bound is the Reuss, series element, uniform stress equation,

$$1/G(\text{lower}) = V_1/G_1 + V_2/G_2 \qquad (2)$$

where 1,2 refer to the amorphous and crystal phases respectively and V is a volume fraction. An equation which encompases both the above and allows interpolation between them is a Halpin–Tsai like composite mixture equation[12]

$$G = (1 + \xi G(\text{upper}))/(\xi + 1/G(\text{lower})) \qquad (3)$$

where G(upper) and G(lower) are given by equations (1) and (2) above and ξ is called variously a contiguity factor, an aspect ratio or a reinforcement factor[10]. Here it is taken simply to be an interpolating factor or mixing parameter. For $\xi \rightarrow 0$ the lower bound is recovered and for $\xi \rightarrow$ infinity the upper bound is approached. A sample calculation is highly instructive. The phase moduli in equations (1) and (2) can be regarded as complex dynamic moduli (G_1^* and G_2^*). Suppose the relaxation is in the amorphous phase and its loss modulus has a value (at some time–temperature point, perhaps at G''_{1max}) of $G''_1 = G'_1/10$, also suppose the crystal modulus has the value $G'_2 = 10G'_1$ but $G''_2 = 0$ (no relaxation process). Then equation (3) can be rationalized into specimen properties G',G''; $J' = G'/(G'^2 + G''^2)$, $J'' = G''/(G'^2 + G''^2)$;

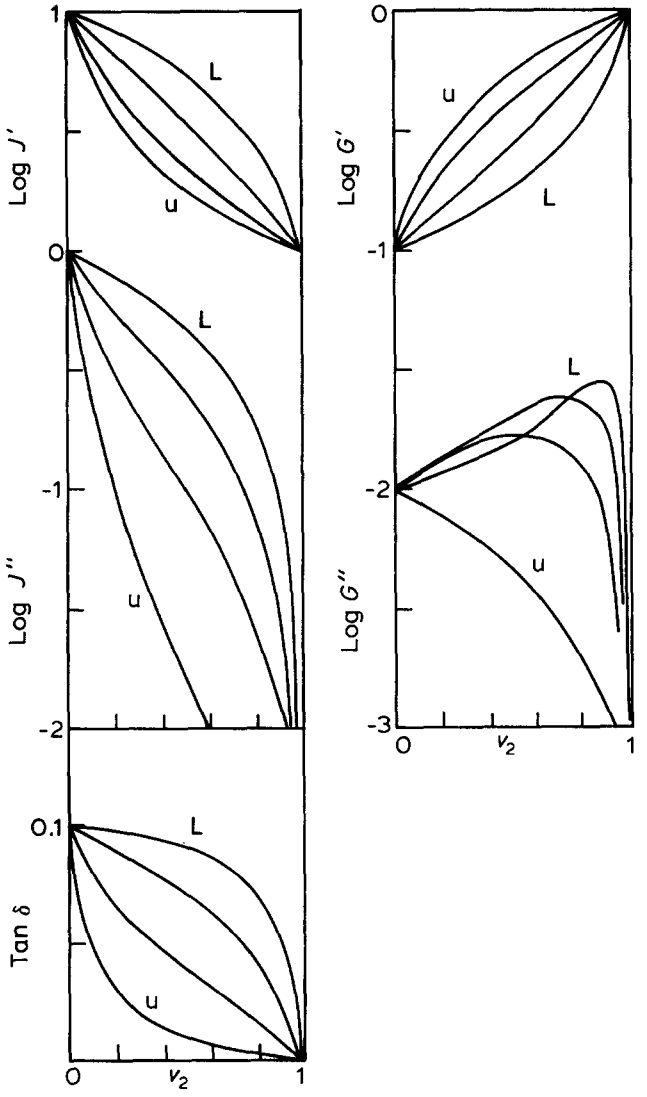

Figure 1 Various measures (J^*, G^*, $\tan\delta$) of relaxation behaviour vs. crystallinity (V_2). Four materials of varying composite system response (values of ξ in Halpin–Tsai equation) are shown. The curve labelled *U* is the Voigt upper bound material ($\xi=\infty$); curve L is the Reuss lower bound material ($\xi=0$), two intermediate values of $\xi=2$, and 10 are also shown. Each material has an amorphous (1) phase relaxation ($G_1''=0.1G_1'$), but none in the crystal (2) fraction ($G_2''=0$, $G_2'=10G_1'$). Notice that for the lower bound and intermediate materials, although the relaxation occurs in the amorphous phase, the specimen loss as measured by G'' *increases* with crystallinity

$\tan\delta = G''/G' = J''/J'$ as a function of crystallinity, V_2 for various values of the mixing parameter. *Figure 1* shows the result. The real components G'. J' are relatively straightforward; they reflect the increase in modulus or decrease in compliance as the stiffer phase increases in content. The loss compliance J'' decreases (for all mixing parameters) with increasing crystallinity and a plot of J'' vs. V_2 would lead to the correct conclusion that the loss process resides in the amorphous fraction. However, for mixing parameters in the lower bound vicinity (small ξ) the loss modulus G'' *increases with crystallinity* over nearly all of the crystallinity range. For such a material a plot of G'' vs. crystallinity would lead to the incorrect conclusion that the loss process resides in the crystal phase if the extreme data points near $V_2=1$ were not available. However, an advantage for plotting J'' may not be supposed. On the contrary, if the relaxation process were in the crystal phase (with a similar ratio of G_2''/G_2'), for near upper bound materials (high ξ) J'' would show anomalous behaviour (decrease in J'' with crystallinity in this case). Since it is not necessarily known what kind of material is being dealt with (high or low ξ) it is clearly not safe to use variation of loss (either G'' or J'') with crystallinity as an indicator for phase assignment. However, for all material types (values of ξ) $\tan\delta$ does show the proper variation and may be used as a diagnostic. A caution should be expressed. Sometimes it is supposed that the relaxation process resides in both phases but with greater strength in one. Notice that *linear* extrapolation to the extremes V_1 or $V_2=0$ from data at intermediate degrees of crystallinity would be an inaccurate procedure for most types of material (values of ξ). The only way to be sure that a prominent relaxation in one phase does or does not have a weaker component in the other phase is to observe whether or not $\tan\delta$ approaches zero as the extreme of $V_2=0$ or 1 is approached. Such degrees of crystallinity may or may not be experimentally accessible for a given polymer. To sum up then, $\tan\delta_{max}$ (but not necessarily G''_{max} or J''_{max}) may usually be expected to correlate directly with phase origin, however plots vs. crystallinity may not be linear.

Mechanical relaxation strength and composite models

An alternative to plotting $\tan\delta_{max}$ vs. crystallinity of course is to plot the unrelaxed and relaxed moduli of each specimen vs. crystallinity and to observe the variation of relaxation strength. This has the advantage of eliminating the possible effects of changes in shapes of peaks with crystallinity on peak heights. However, it requires more analysis of the data to establish these limiting moduli for each specimen. Mechanically, this has not often been undertaken traditionally, especially in the studies of dynamic modulus variation with temperature at a single frequency (isochronal scans). It is common in dielectric measurements to establish the limiting constants. It will be seen that such analysis is practical in isochronal mechanical studies as well and limiting moduli and dielectric constant variation will be emphasized as indicators of phase origin.

It is apparent that if relaxation strength data is to be extrapolated beyond the experimentally determined range or the data used to determine phase moduli and phase relaxation strength, improved mixing equations are required. Further, extensive experimental data that would allow assessment of the validity of proposed equations is a necessity. At present, the appropriate data is rather minimal but it will be stressed in further discussions.

There has been significant progress in developing improved mixing equations. In any such mixture modelling there are two major problems. First, proper local continuity across phase boundaries must be incorporated. Second, the materials are polycrystalline with a distribution of crystal orientations. The Voigt equation incorporates appropriate boundary conditions (continuous strains, additive forces) for a layered structure of crystals and amorphous phases when deformed in directions within the layers but not for other crystal orientations. Conversely the Reuss equation has boundary conditions (continuous stress, additive displacements) appropriate for stress applied normal to the crystal surfaces in the layered structure but not for other orientations. Both equations neglect the effects of lateral

contractions (Poisson's ratio). In addition it should be recognized that the crystal modulus in the normal direction is quite different from that within the lamellar layer directions. More properly an application of the Voigt, Reuss equations as bounds should use different values of G_2 in equations (1) and (2).

Halpin and Kardos[5] have attempted to remove these difficulties by modelling the system as a short fibre composite. It is laid-up from randomly oriented plies that individually are unidirectional short fibre composites. The Halpin–Tsai equation[12] which has been successfully used to describe short fibre composites is used to describe the response of a single layer. Then, composite lamination theory is used to compute the response of multiple layers, and thereby average over various crystal orientations. In supplying parameters for the Halpin–Tsai equation an upper bound average of the crystal *a* and *c* directions was used to compute the transverse fibre response. The averaging over crystal orientations accomplished by the lay-up is actually only two-dimensional rather than three. The uncertainties introduced by these approximations results in upper bound-like character to the resulting equations. They are a great improvement over the Voigt equation but nevertheless are still an upper bound-like approximation. The application to experimental data has been discussed by Kardos and Raisoni[6] and by Boyd[13].

Another application of a composite approach has been made by Wang[7–9]. Locally, the crystal amorphous response is calculated using a fibre composite equation due to Hill[14] and Hermans[15]. In accomplishing this the elastic constants of the crystal were averaged via a Voigt average before inserting in the composite equation. In an application to spherulitic polymers[8], the local response modelled this way was used to describe the elastic properties of a sphere (which becomes elastically anisotropic in the radial and tangential directions). The solution for the response of such a sphere imbedded in a continuous elastic medium is used to compute the moduli of the spherulitic aggregate. Thus, unlike the Halpin–Kardos model this is a true three dimensional model. Like the Halpin–Kardos model the (extreme) crystal transverse (*a*,*c*) elastic constant anisotropy muxt be pre-averaged (and both use the Voigt average).

More recently it has been shown that if the local morphology is lamellar (extended stacked thin plate-like crystals separated by amorphous layers) bounds on the moduli (both upper and lower) that are much tighter than the Reuss–Voigt extremes can be derived[16]. The treatment is based on using lamination theory to formulate a local response matrix (either stiffness or compliance) for a local region comprised of a number of lamellae. Each matrix simultaneously incorporates the continuity of stress and additivity of displacements normal to the lamellar surfaces and continuity of strain and additive forces in the lamellar planes. The effects of lateral contractions are incorporated as well. The anisotropy of the crystal phase is retained. Averaging of the stiffness matrix under constant strain over various crystal orientations leads to upper bounds on the engineering moduli and averaging of the compliance matrix under constant stress leads to lower bounds. Sample calculations[16] comparing the lamellar bounds with the Reuss–Voigt bounds are shown in *Figure 2*. The lamellar bounds are much tighter and the divergence of bounds as V_2 approaches one is delayed to be very high crystallinity whereas it is evident over all of the crystallinity range for the Reuss–Voigt bounds. Notice also that the lamellar bounds lie closer to the Reuss lower bound than to the Voigt upper bound. The Reuss–Voigt bounds have simple curvature (in Log modulus), positive and negative respectively, over the entire V_2 range whereas the lamellar bounds are more complex and each can have both upward and downward curvature. The application of the lamellar bounds to actual systems will be discussed below.

Dielectric relaxation strength and composite models

The above comments on mechanical behaviour, also apply to dielectric measurements. If it is desired to determine phase dielectric constants from specimen values or extrapolate data vs. crystallinity, a mixture equation is necessary. The problem is not as severe as in the mechanical case because the phase values are often not as disparate. The simple mixture equations for dielectric constant, analogous to the Reuss and Voigt equations,

$$\varepsilon = V_1\varepsilon_1 + V_2\varepsilon_2 \tag{4}$$

$$1/\varepsilon = V_1/\varepsilon_1 + V_2/\varepsilon_2 \tag{5}$$

are upper and lower bounds. Hashin and Shtrikman[17] have derived tighter bounds for a mixture of unspecified morphology by using a better variational principle. In the case of lamellar morphology, a treatment paralleling that of the mechanical case is possible[18]. These bounds are much better than the ones in equations (4) and (5), and, although they result from constant electric and displacement field averaging over crystal orientations, they are considerably tighter than the Hashin–Shtrikman bounds. The phase geometry specification is more important than the better variational principle of the latter. For a number of actual examples the lamellar bounds are tight enough to specify the mixture dielectric constant with experimentally practical accuracy. Illustrative calculations using the various bounds are shown in *Figure 3*.

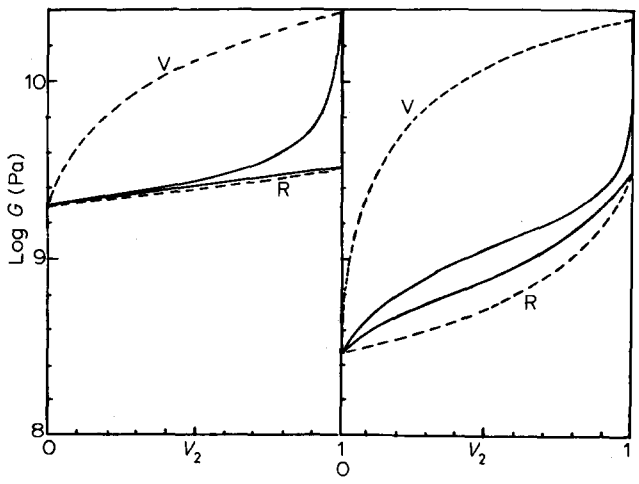

Figure 2 Lamellar bounds. Calculated bounds (*versus* crystallinity) on the shear modulus of a macroscopically isotropic PE specimen (Boyd[16]). Two cases are shown, amorphous phase modulus $G_1 = 2.0$, 0.3 GPa. Voigt and Reuss bounds (dashed curves) are also shown. (Divergence of bounds at high crystallinity is due to mechanical anisotropy of the crystal)

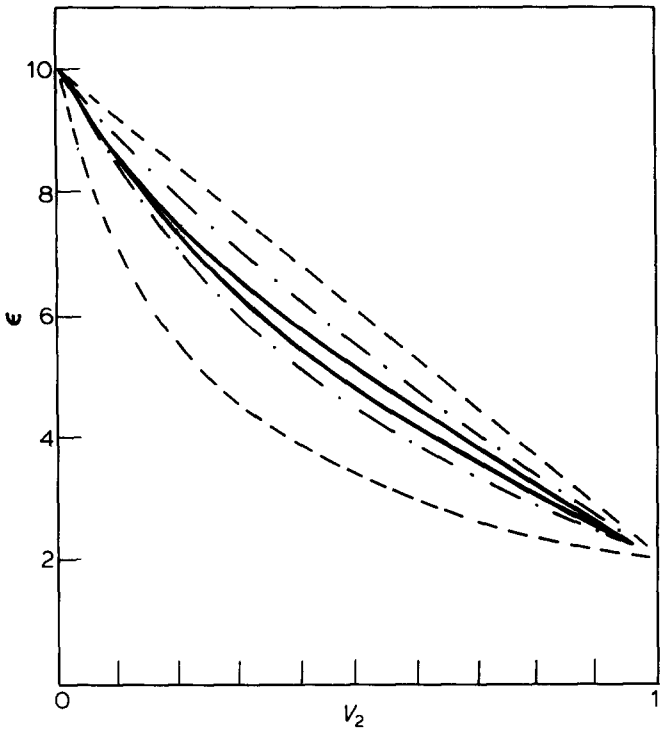

Figure 3 Lamellar bounds (Boyd[18]) on dielectric constant *versus* crystallinity (—). Hashin and Shtrikman[17] bounds (-·-·-) and simple 'parallel' and 'series' mixing rules (---) are also shown. (Dielectric constant of amorphous fraction=10, crystal=2)

RELAXATIONS IN LOW CRYSTALLINITY POLYMERS

As an illustrative example, the relaxation behaviour of PET, a system for which both mechanical and dielectric data are available, is reviewed. In *Figure 4* the shear modulus data of Illers and Breuer[19] covering specimens of crystallinity varying from 0–~50% (prepared by isothermal crystallization of amorphous PET at various temperatures, T_c) is shown in the glass transition region (the α_a relaxation). The relaxation in the completely amorphous sample has the character of a typical glass transition, the modulus dropping orders of magnitude (presumably towards some temporary rubbery plateau characteristic of an uncrosslinked viscoelastic melt). The specimens of higher crystallinity obviously have the character expected of a composite system in which one phase softens in a manner analogous to the completely amorphous specimen but where the other phase does not relax. There are several important further observations. First, the temperature of the process ($T_{max}(G'')$ for instance) is displaced upward in the semicrystalline specimens. Second, the width of the process is much broader in the crystalline ones. These effects are to be attributed to the effect of the crystals in restricting the generalized long-range segmental motions in the amorphous phase that are characteristic of a glass transition. The amount of shift of T_{max} depends on the crystallization temperature, going through a maximum at $T_c = 150°C$ (~30% crystallinity) and becoming smaller in the higher crystallinity specimens. Illers and Breuer[19] point out that low-angle X-ray results[20] indicate that the higher crystallinity specimens have *both* thicker crystals *and* thicker amorphous layers than the lower crystallinity specimens. The thicker amorphous layers would lead to a lessening of the constraints imposed by the crystal surfaces. It is also to be noted in *Figure 4* that log G' turns down at a temperature corresponding to T_c in the intermediate crystallinity samples. This is no doubt due to recrystallization and indicates a lessening of constraint by the crystals. Apparently the smaller crystals formed during original crystallization at lower T_c melt in an isochronal upward temperature scan before the new larger crystals form.

Dielectric experiments[21–23] show similar results but with somewhat more detail since multiple frequency measurements are practical. First it is desirable to briefly review the dielectric behaviour of completely amorphous polymers in the glass–rubber relaxation region[24,25]. This relaxation is comparatively rather narrow in the frequency domain but skewed toward the high frequency side. The shape is well accounted for by the Havriliak–Negami (HN) phenomenological equation[24] for the complex dielectric constant, ε^*,

$$\varepsilon^* = \varepsilon_U + (\varepsilon_R - \varepsilon_U)(1 + (i\omega\tau_0)^{\bar{\alpha}})^{-\bar{\beta}} \qquad (6)$$

that generalizes the Cole–Cole equation[26] (which admits symmetrical broadening about the central relaxation time, τ_0, through $\bar{\alpha} < 1$) and the Davidson–Cole equation[27] (which incorporates asymmetric high frequency side broadening through $\bar{\beta} < 1$). Relaxed and unrelaxed values of the dielectric constant are designated by the subscripts R and U respectively. Typically, $\bar{\alpha}$ is ≈ 0.8

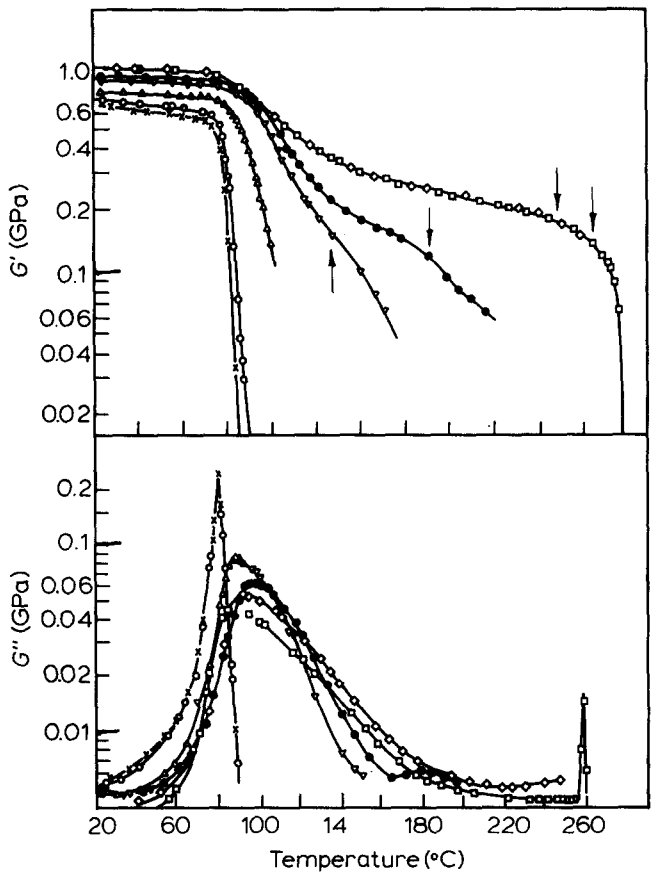

Figure 4 Complex shear modulus of PET (~1 Hz, torsion pendulum, Illers and Breuer[19]), *versus* temperature in the glass–rubber relaxation region for specimens of various crystallinities obtained by isothermal crystallization (□): 46%; (◇), 40%; (●), 33%; (▽), 26%; (△), 16%; (□), 2–3%; (x), 0%. Crystallization temperatures (T_c) are shown for higher crystallinites by vertical arrows

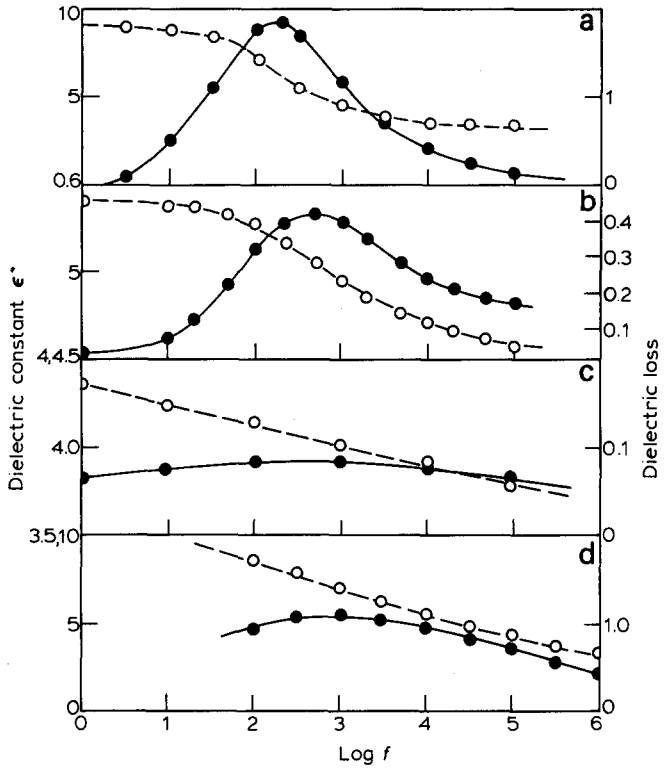

Figure 5 Dielectric constant (○), and loss (●), *versus* log frequency of completely amorphous and semi-crystalline polymers compared in the glass–rubber relaxation region. (a) PVAc (62.5°C) (Ishida[28]), is a typical completely amorphous polymer. (b) (91.3°C) PET(A) is a completely amorphous PET and behaves similarly to PVAc. (c) PET(XL) (109.3°C) is a ~50% crystalline PET and has a much broader more symmetric loss *versus* frequency curve (PET data from Coburn and Boyd[23]). (d) PVC (101.5°C) is a low crystallinity polymer whose extent of crystallinity has not been well understood, however its loss behaviour (Ishida[34]), is seen to be more typical of a semi-crystalline polymer than a wholly amorphous one

(slight symmetric broadening) and $\bar{\beta}$ is ≈ 0.5 (significant high frequency skewing)[24,25]. Data for polyvinylacetate (PVAc)[28] which is typical of such polymers is shown in *Figure 5* (dielectric constant and loss) and *Figure 6* (Cole–Cole plot). Data for amorphous PET is shown in *Figure 5* and *Figure 6*. It is also seen to be typical of amorphous polymers. However, the data for a crystalline specimen (*Figure 5* and *Figure 6*) is seen to be significantly different. The loss region has been shifted ≈ 18 degrees to higher temperature and it is greatly broadened compared to the amorphous specimen. The shape now appears to be nearly symmetric. The Cole–Cole equation ($\bar{\beta} = 1$) fits the data. Width parameters ($\bar{\alpha}$) in the range 0.2–0.3 are found. In a series of samples of varying crystallinity there does not seem to be a correlation between the degree of crystallinity, once the latter is present, and the degree of broadening[23].

The glass transition and the relaxation behaviour associated with it in amorphous polymers is very sensitive to the addition of small amounts of diluents. The relaxation is shifted to lower temperature isochronally or higher frequency isothermally. The usual explanation is that since the diluent molecules are small and mobile, they act to effectively increase the available free volume for segmental motion and hence speed it up. Similar plasticizing effects on the glass–rubber relaxation in PET are observed. *Figure 7* shows the effect of dioxane in displacing the α_a peak to a lower temperature.

The dynamic behaviour of the β subglass relaxation in PET is quite different from that of the α_a glass–rubber relaxation. In *Figure 8* the dynamic shear modulus vs. temperature for the same specimens as in *Figure 4* are shown in the β region. It is apparent that the shape and location of the β process are insensitive to either the presence or degree of crystallinity. Dielectric results show similar behaviour[23]. The insensitivity of the dynamics of this subglass process to the presence of the crystal phase is easily rationalized if the process is supposed to be associated with molecular motions that are of a localized character. This would be in contrast to the long-range generalized segmental motions underlying the glass–rubber relaxation that are sensitive to the connections to the crystals. The lack of variation of the magnitude of G''_{max} with crystallinity evident in *Figure 8* as will be seen below is due to the effects discussed in the previous section concerning the type of composite behaviour (*Figure 1*) and is not an indicator of phase origin.

A further important feature of the β process concerns its shape in isochronal temperature scans. Dielectric measurements show that the β process narrows strongly in the frequency domain ($\bar{\alpha}$ increasing) with increasing temperature. This narrowing is important because of the effect it has on isochronal temperature scans. A process having a relaxation time distribution symmetric in $\log \tau$ and having Arrhenius dependence of each $\log \tau$ (and thus a frequency domain shape independent of temperature) will have an isochronal loss scan symmetric in $1/T$ (since $\log \tau = A/T + B$). Therefore the loss will be skewed toward high temperature in an isochronal plot vs. T. The effect of narrowing of the distribution of τ's with increasing temperature is to sharpen the high temperature side,

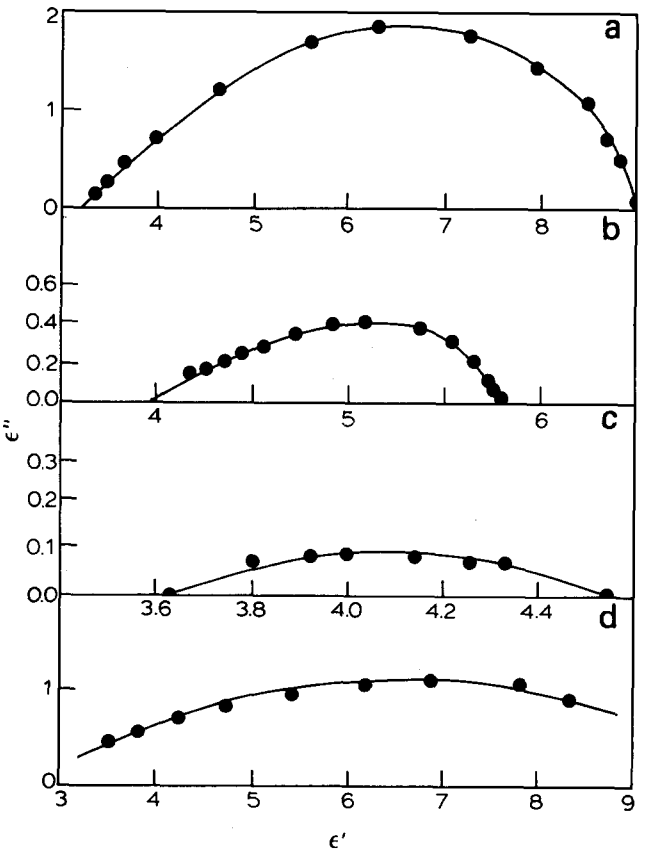

Figure 6 Cole–Cole plots for the same polymers as in *Figure 5*

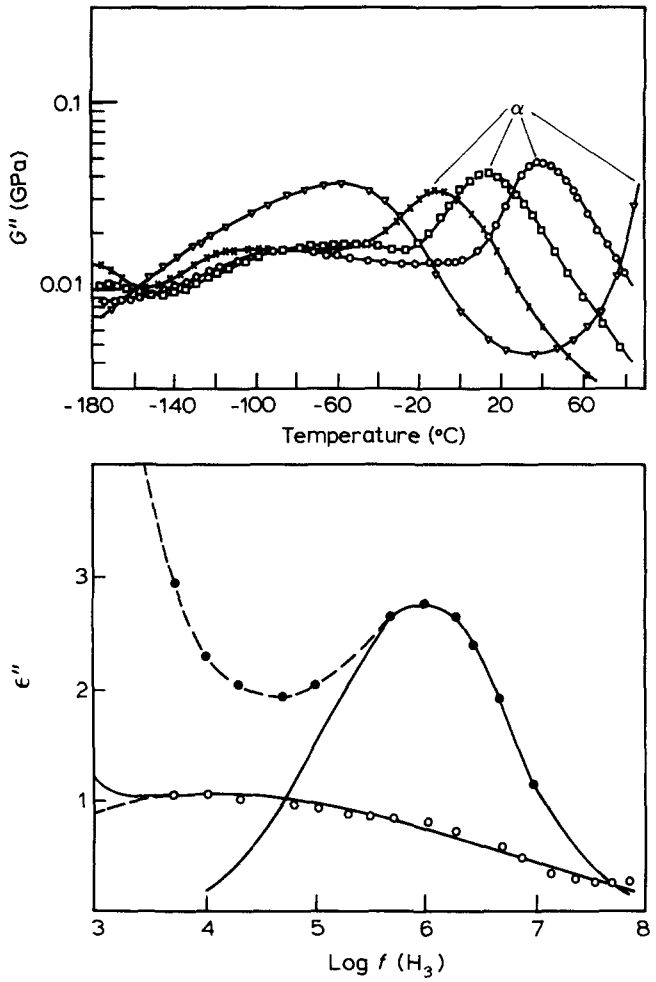

Figure 7 (a) The effect of plasticizer on the glass–rubber α_a and β relaxations. (a) PET (shear loss modulus, torsion pendulum, Illers and Breuer[19]), ((▽), 0%; (○), 4.5%; (□), 10.1%; (x), 17.2% dioxane). (b) Nylon 6-6 (dielectric loss, (○), dry, 82°C; (●), 2.3% water, 80°C; Fuoss–Kirkwood width parameter=0.21 dry, =0.57 2.3% water, upturn at low frequency is due to D. C. conductance). (Boyd[37])

compared to the low, of an isochronal loss scan. If the temperature narrowing is sufficiently great it can lead to skewing toward low temperature in such plots. The difference in isochronal shapes for the α_a and β processes (mechanical process, *Figure 4* vs. *Figure 8*) is due to just this effect. For the α_a process, the width parameter is nearly independent of temperature and log G'' in *Figure 4* is skewed toward high temperature whereas for the β process the distribution width narrows with increasing temperature and log G'' is skewed toward low temperature in *Figure 8*. Unfortunately, low temperature skewing of mechanical single frequency isochronal temperature scans of loss like that exhibited by the β subglass process (*Figure 8*) has often been invoked as evidence for complex structure due to competing overlapping distinct mechanisms. The fact that the β process here has virtually the same shape in the completely amorphous and crystalline specimens rules out making a case for complex shape due to competing amorphous and crystalline mechanisms. Rather, the shape is easily accounted for as a phenonemological effect due to narrowing of the relaxation time distribution with increasing temperature. Close inspection of *Figure 8* reveals some apparent structure to log G'' as a slight low temperature side inflection. This also has a simple phenonemological explanation. It is due to a cut-off or decrease in the rate of broadening of the relaxation time distribution with lowering temperature. More substance can be given to these statements via the following calculation.

It is common in dielectric studies to fit experimental data with empirical equations. Although traditionally not as common this is quite feasible for mechanical relaxation studies as well, including isochronal scans. For example, the Havriliak–Negami equation can be modified for a relaxation rather than a retardation process as,

$$G^* = G_R + (G_U - G_R)[1 - (1 + (i\omega\tau_0)^{\bar{\alpha}})^{-\bar{\beta}}] \qquad (7)$$

where for example G^* is the complex shear modulus, U and R designate its unrelaxed and relaxed values and the other parameters have the same meaning and effect as in equation (6). This equation can be used to fit isochronal mechanical scan. For PET two such terms are necessary, one each for the α_a and β processes. Because the dielectric frequency domain data appears rather symmetric it is reasonable mechanically to simplify the fitting by setting $\bar{\beta} = 1$ for both processes (and thereby use the Cole–Cole equation analogy). The results[29] of fitting the highest crystallinity specimen of *Figure 4* and *Figure 8* are displayed in *Figure 9*. The parameters were determined via nonlinear regression analysis. The shape of the β process log G'' vs. T curve is reproduced very well. The fitting serves to establish the unrelaxed and relaxed moduli for the two processes and hence the relaxation strengths for this specimen. This is important since G' through and above the α_a process is strongly temperatue dependent and it is not obvious by inspection how much of this is due to relaxation and how much is due to temperature dependence of G_R.

Although the morphological assignment of the α_a process is not in doubt (due the availability of the completely amorphous material) it is instructive to plot relaxation strength vs. crystallinity to establish the kind of composite behaviour experienced in this system. This is useful in quantifying the degree of softening of the amorphous phase, in deciding whether G_1 (amorphous phase modulus) is independent of crystallinity once the latter is present and in developing experience for comparison with systems where the completely amorphous

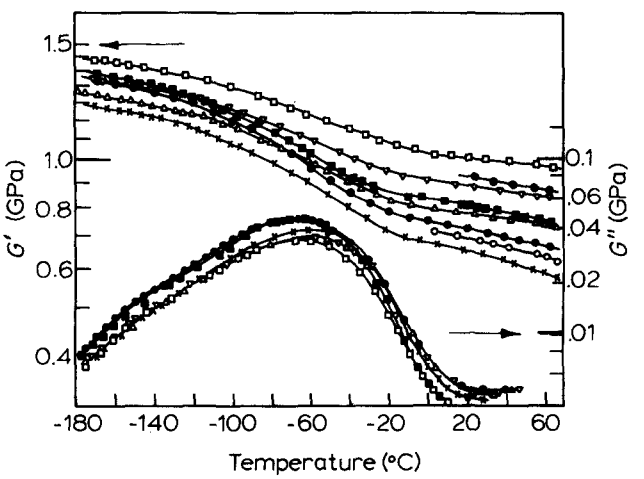

Figure 8 Complex shear modulus of PET (≈1 Hz, torsion pendulum, Illers and Breuer[19], for the same specimens as in *Figure 4* but in the β subglass relaxation region

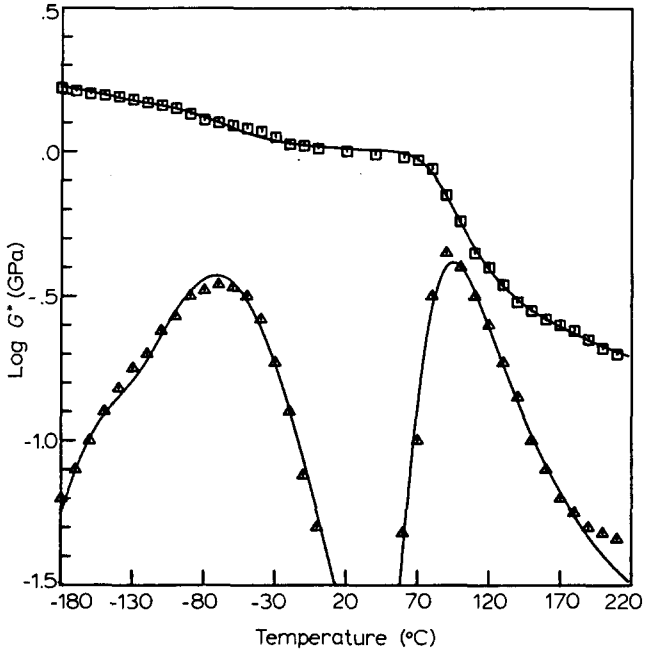

Figure 9 Cole–Cole equation fit of the complex shear modulus of semi-crystalline PET (46% sample of *Figure 4* and *Figure 10*). The curves were calculated (Boyd[29]) using equation (7) of text using parameters determined by nonlinear regression fit of the experimental points. The log G'' curve is displaced 1.0 upward in plotting

material is not available. In *Figure 10* the limiting moduli for the specimens of *Figure 4* are plotted vs. crystallinity. Because of the recrystallization at T_c it is only possible to determine the relaxed modulus for the α_a at the three highest crystallinities. The curves in *Figure 10* were calculated[30] using the lamellar *lower* bound equations[29]. The required inputs are the elastic constant matrix for the crystal and the shear modulus (G_1) and Poisson's ration (ν_1) of the amorphous fraction. The crystal elastic constants were estimated (and no relaxation process was incorporated) and ν_1 was set to 0.33. The parameter G_1 was assumed to be independent of crystallinity and adjusted to fit each curve. For $G_U(\beta)$ a single value of G_1 serves quite well to fit the data at all crystallinities. The same is true for $G_R(\beta) = G_U(\alpha_a)$. For the relaxed moduli for the α_a process, $G_R(\alpha_a)$, it appears that although a single value of $G_1 = 0.10$ GPa serves to fit the two highest crystallinities (40, 46%), a somewhat lower value is required to fit the 32% crystallinity specimen. When the lamellar *upper* bound equations are used, it is found that poor fits of the specimen $G_U(\beta)$ and $G_R(\beta)$ ($= G_U(\alpha_a)$) values are obtained, the aggregate average 100% crystallinity shear modulus is calculated to be much too high (high crystallinity upturn like that in *Figure 2*). It is also found that *no* value of G_1 will fit the relaxed α_a process values, the curve for $G_1 = 0$ being too high. If G(upper) and G(lower) in equation (3) are taken to be the lamellar upper and lower bounds rather than the Voigt–Reuss bounds (equations (1) and (2)) then it is found that ξ must be ≈ 100 or less in order to find a G_1 value (≈ 0.005 GPa) that will fit $G_R(\alpha_a)$. The conclusions then are the following. For the β process the lamellar bounds serve to define an amorphous phase G_1 value for the unrelaxed and relaxed state. However for the α_a process the relaxed amorphous phase modulus is not well defined but probably lies between 100 and 5 MPa (at 160°C) and may depend somewhat on the degree of crystallinity. Near lamellar lower bound behaviour appears to give a much better representation of crystallinity variation of modulus than the lamellar upper bound.

It is seen in *Figure 10* that amorphous phase origin is well accommodated, even demanded, by the data and curves for the β process (i.e. vanishing relaxation strength as V_2 approaches one). In contrast G''_{max} for the β process shows (*Figure 8*) almost no variation at all with crystallinity. This is in consequence of, and illustrative of, the considerations discussed above under morphological assignment. The material behaves in a lower bound-like manner (see *Figure 1*). It is also to be noted that tan δ_{max} derived from the data of *Figure 8* does show decrease with increasing crystallinity, in agreement with the conclusions derived from *Figure 1*.

The specimen dielectric relaxation strengths for the α_a and β processes in PET are plotted vs. crystallinity in *Figure 11*. These results[23] take advantage of higher crystallinities (via crystallization under high pressure) than available previously[19,21,22]. It is seen that amorphous phase origin is indicated for both the α_a and β processes. The dielectric relaxation strengths permit the discussion of a further important effect of the crystals on the amorphous phase. The strengths are a measure of the degree to which the interaction of the amorphous fraction with the crystals affects availability of amorphous chain configurations. The dielectric relaxation strength is a measure of the ability of a given dipole to relax over all spatial directions and of the intramolecular correlation between dipoles. Reduction in availability of amorphous chain configurations could restrict the spatial ability to relax and alter intramolecular correlation. Making this assessment requires the relaxation strength in the amorphous phase. When the relaxed dielectric constant of the

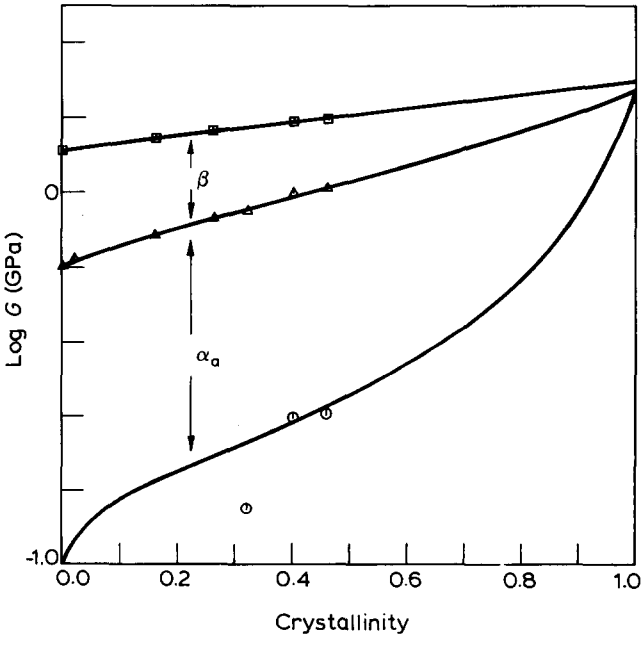

Figure 10 Relaxation strengths of the mechanical α_a and β processes in PET *versus* crystallinity. The points are the relaxed and unrelaxed shear moduli of the two processes determined by phenomenological fitting of the data of *Figure 4* and *Figure 10*. The curves are calculated ones using the lamellar lower bound equations (Boyd[29]) and utilize an adjustable amorphous phase modulus

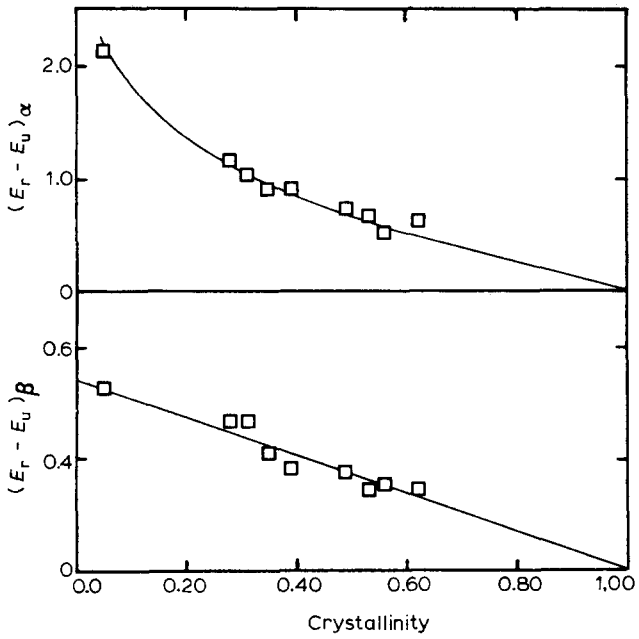

Figure 11 Strengths of the dielectric α_a and β processes in PET *versus* crystallinity. Relaxed and unrelaxed dielectric constants of the two processes determined from phenomenological fits (Coburn and Boyd[23])

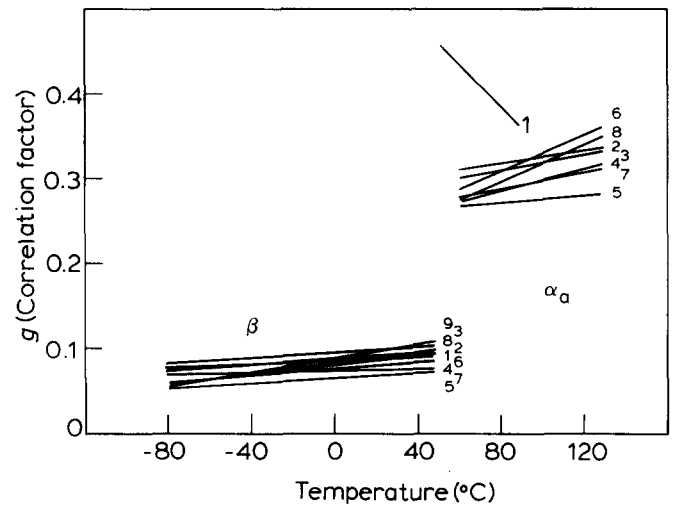

Figure 12 Kirkwood–Onsager dielectric correlation factor, g, for the amorphous fraction *versus* temperature in PET (Coburn and Boyd[23]). (Crystallinity, 1≈0%, 2=28%, 3=31%, 4=34%, 5=39%, 6=49%, 7=53%, 8=56%, 9=63%). Correlation factors were calculated from amorphous phase dielectric constant calculated in turn from specimen values using lamellar bounding equations

amorphous fraction in a crystalline specimen is back-calculated from a measured specimen value using the lamellar bounding relations[18] the value is found to be closely bounded. For the α_a process the values found are lower than the measured value for the wholly amorphous PET. The results of converting the amorphous phase relaxed dielectric constants into apparent dipole correlation factors (via the Kirkwood–Onsager equation) is shown in *Figure 12*. for the $\alpha_a + \beta$ processes there is a reduction in 'g' with crystallinity that is most significant with the onset of the presence of the crystals. This is consistent with the behaviour of the dynamic parameters (log τ_o, $\bar{\alpha}$) discussed above. For the β process the correlation factors are seen to be quite insensitive to the presence and degree of crystallinity, a result again consistent with the dynamics of that process.

Isotactic polystyrene (iPS) behaves in a manner similar to PET in that a crystalline specimen shows mechanically an α_a relaxation that is much broader (and at a slightly higher temperature isochronally) than in a quenched completely amorphous isotactic specimen[31,32].

Poly(vinyl chloride) (PVC) is an interesting case because its classification as a crystalline polymer has been subject to much uncertainty over the years and, if it is to be so considered, its morphology and level of crystallinity have not been well understood. It is clear however that its dielectric loss spectrum[33,34] belongs to the broad relatively symmetric type characteristic of crystalline polymers rather than the more narrow high frequency skewed type associated with wholly amorphous polymers (see *Figure 5* and *Figure 6*). This observation seems to be in accord with recent studies of its solid-state structure[35].

RELAXATIONS IN MEDIUM CRYSTALLINITY POLYMERS

These materials show a strong relaxation process that would appear to have the same interpretation as in the low crystallinity polymers of the preceding section (i.e. the glass–rubber relaxation of the amorphous phase). However the direct comparison of the relaxation behaviour of the completely amorphous material with the semi-crystalline one is not possible because of the unattainability of the former. It is important to show as directly as possible in at least a few cases that this morphological assignment is a correct concept. Another way to create a completely amorphous material (rather than by quenching) is by melting. If the same relaxation process in the solid can be observed in the melt this would also directly show the correspondence between the relaxation in free amorphous condition and that in the amorphous fraction in the solid. In the case of the aliphatic polyamides this is possible. Although the loss process moves to higher frequency with increasing temperature, by making measurements at high frequencies (approaching 10 GHz), it is possible in nylon 610 to follow the α_a process into the melt[36]. There is an abrupt increase in relaxation strength on melting, a result of the conversion of the entire material to the amorphous condition (see *Figure 13*). The location of ($\log f_{max}$ vs. $1/T$) and the width of the process (*Figure 13*) extrapolate smoothly into the melt showing that the same processes are operative in both solid and melt. Based on

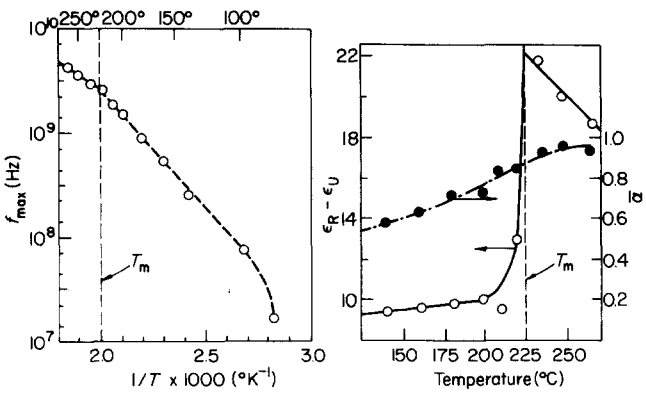

Figure 13 Effect of melting on the dielectric glass–rubber relaxation in nylon 6-10 (Boyd and Porter[36]). The relaxation location (as log $f$max vs. $1/T$) and breadth (as Cole–Cole α vs. temperature) are tracked through the melting point (T_m). Relaxation strength undergoes a large increase on melting

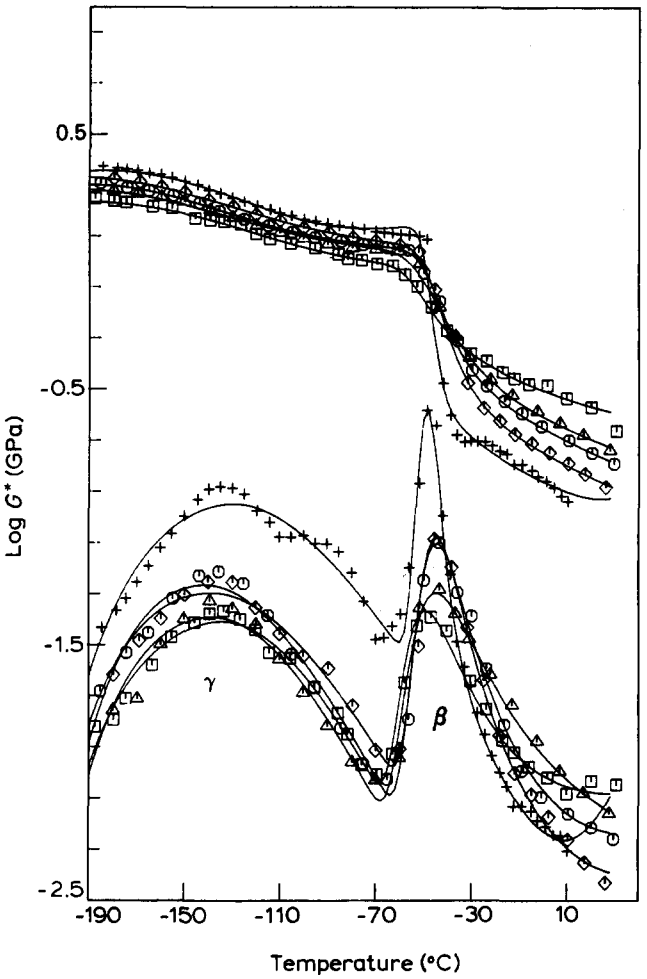

Figure 14 Complex shear modulus of aliphatic copolyesters of varying crystallinity *versus* temperature (torsion pendulum, ≈1 Hz, Boyd and Aylwin[44]). (□, 60%; △, 44%; ○, 36%; ◇, 30%; +, 20% crystallinity; completely amorphous '6B-6' homopolymer is not shown). The curves are calculated from the mechanical Cole–Cole equation using parameters obtained from optimizing the fit to the data

the results of comparing the completely amorphous relaxation with that in the crystalline solid in PET an abrupt narrowing and some shift to higher frequency on melting should be expected. However, it is to be observed (*Figure 13*) there is strong narrowing of the relaxation in the solid with increasing temperature. In fact, just below the melting point the process is already so narrow (Cole–Cole width parameter ≈0.8–0.9) that further narrowing on melting is perforce negligible. As a corollary, the lack of amorphous phase constraint in the solid at high temperature near the melting point implied by the narrowing also implies very similar loss peak location compared to the melt. However since the width in the solid is strongly temperature dependent it is quite reasonable to suppose that both the width and location of the loss peak in the supercooled melt and the solid would diverge as temperature is lowered far below the melting point. At the lower end of the temperature range where the α_a process in the nylons can be resolved the width parameters are similar to PET, i.e. ≈0.2 for the Fuoss–Kirkwood width parameter. As in PET the α_a relaxation is very sensitive to plasticization[37,38]. Addition of small amounts of water or alcohols (which are soluble in the amorphous fraction by virtue of hydrogen bonding) moves the loss peak to higher frequency isothermally and dramatically narrows it (*Figure 7*), a result consistent with increased free volume reducing the constraints imposed by the crystals.

Aliphatic polyesters are interesting systems that have been the subject of recent relaxation studies[39–45] after a long period of relative obscurity. Like PET and the aliphatic polyamides they show a well-developed process ostensibly to be attributed to the amorphous phase glass–rubber relaxation. Although the low melting points (≈50–60°C) tend to interfere with the observation of a possible crystalline α process there are good indications that one occurs in some members of the family[40]. Therefore the notation β is adopted for the apparent glass–rubber relaxation. A prominent subglass relaxation, therefore labelled γ, also occurs, and, as its behaviour is very similar to the γ process in polyethylenes, a notational correspondence is preserved. Wholly amorphous states are not achieved by quenching. However it has been possible to vary crystallinity over the range 0–60% by copolymerization with a non-crystallizable diol[42–44]. The homopolymer of 1,6-hexanediol condensed with adipic acid ('6-6' polyester) is ≈60% crystalline but the homopolymer of 2,5-hexandiol with adipic acid ('6B-6') polyester) is completely amorphous. At ratios of 1,6 hexanediol/2,5 hexanediol above 50%, crystallinity appears and can be controlled over the range 0–60% by varying the ratio of diols. Mechanical relaxation behaviour[44] of the above copolymers is shown in *Figure 14*. Mechanical and dielectric relaxation strength variation with crystallinity in the copolymers shows that the β relaxation is indeed the glass–rubber relaxation in the amorphous fraction. As in PET, the immobilization of the amorphous fraction by the presence of the crystals is quite dramatic. The 6B-6 homopolymer has a dielectric relaxation frequency domain shape very similar to other wholly amorphous polymer glass–rubber relaxations ($\bar{\beta}$ HN width parameter, 0.4–0.5, $\bar{\alpha}$, 0.8–0.9). All of the crystalline polymers in the copolymer series appear to have symmetric frequency domain losses (HN $\bar{\beta} = 1.0$) but are quite broad and the width increases with degree of crystallinity (see *Figure 15*). The widths for the β process are also seen to be temperature dependent, narrowing with increasing temperature. The width behaviour is somewhat different than that of PET where α_a tends to be independent of crystallinity and temperature once the crystals are present. The widths, expressed as the distributions of relaxation times, are shown in *Figure 16*. The mechanical relaxation process shows similar behaviour. In fact, the mechanical version of the Cole–Cole equation (equation (7), $\bar{\beta} = 1$) was found to fit the mechanical β and γ processes (*Figure 14*) and values of $\bar{\alpha}$ and τ_0 found from non-linear regression analysis[30] are similar to those found dielectrically. The limiting moduli are of course unrelated to the limiting dielectric constants.

The γ process in the aliphatic polyesters has also been assigned to the amorphous fraction. However the variation of relaxation strength with crystallinity is more complex because the chemical composition is also changing (via the mole ratio of diols). The 6B units contribute less to the strength than the 6 units. The dynamics of the γ process depend on the presence of the crystalline fraction in a very different way from the β glass–rubber relaxation but in a manner similar to the subglass process in PET. That is, as is to be seen in *Figure 14* and *Figure 17* both the shape and location of the process are insensitive to the presence of the crystalline fraction.

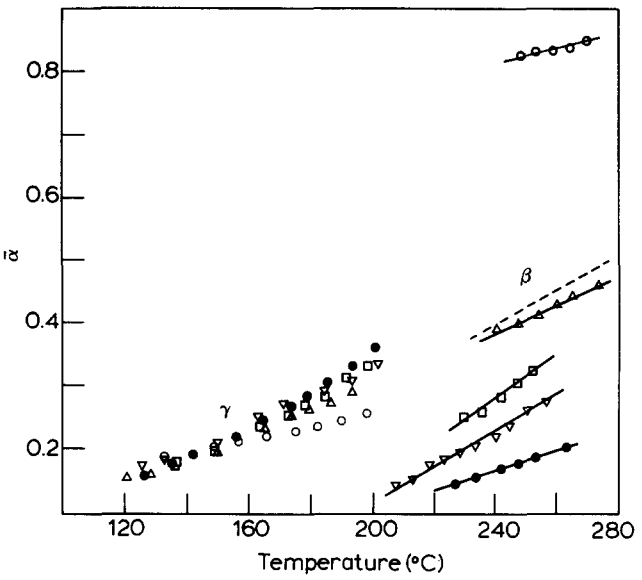

Figure 15 Dielectric relaxation width (Cole–Cole $\bar{\alpha}$) *versus* temperature for aliphatic copolyesters of various crystallinities (●), 60%; (▽), 44%; (□), 36%; (△), 20%; (○), 0%) (Boyd and Aylwin[43]). Both β (glass–rubber relaxation) and γ processes are shown. For the completely amorphous polymer β process the Havriliak–Negami equation is necessary and β for 0% sample is shown (---)

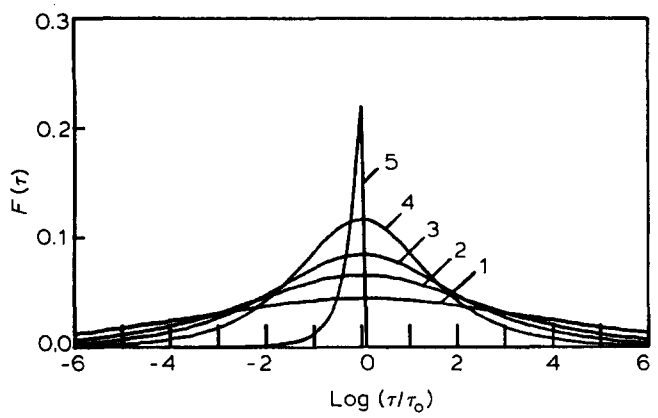

Figure 16 Distribution of dielectric relaxation times *versus* log τ for the β process in aliphatic copolyesters of various crystallinities (1=60%; 2=44%, 3=36%, 4=20%, 5=0%) (Boyd and Aylwin[43])

The dielectric relaxation strengths of the β process in the aliphatic polyesters again (see PET) permit the discussion of the effect of the crystals on amorphous chain configurational behaviour. The result of converting the amorphous phase relaxed dielectric constants into apparent dipole correlation factors is shown in *Figure 18* for the copolymer series. A similar plot comparing the solids and melts of 6-6, 5-7 and 6-10 polyesters is also displayed. The similarity of the values among the latter polymers shows that the correlation factor is not dominated by intramolecular correlation effects. Rather the lower more strongly temperature dependent values for the β ($+\gamma$) processes in the solids compared to the melts are the result of restriction on ability to spatially reorient. This in turn is the result of reduction in availability of amorphous phase configurations engendered by the presence of the crystals. The differences in the correlation factors for the γ process among the specimens in *Figure 18* are due to variation in

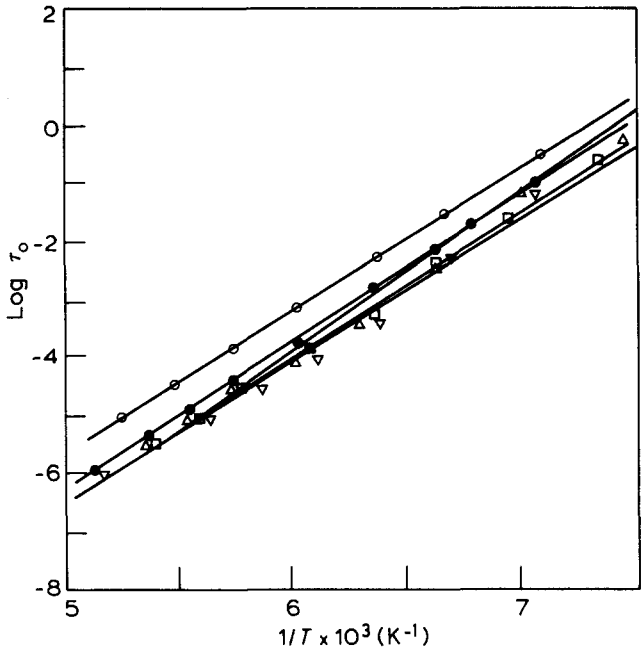

Figure 17 Loss map (log τ_0, Cole–Cole central relaxation time, *versus* $1/T$) for γ process in aliphatic copolyesters (same samples as in *Figure 15*, Boyd and Aylwin[43])

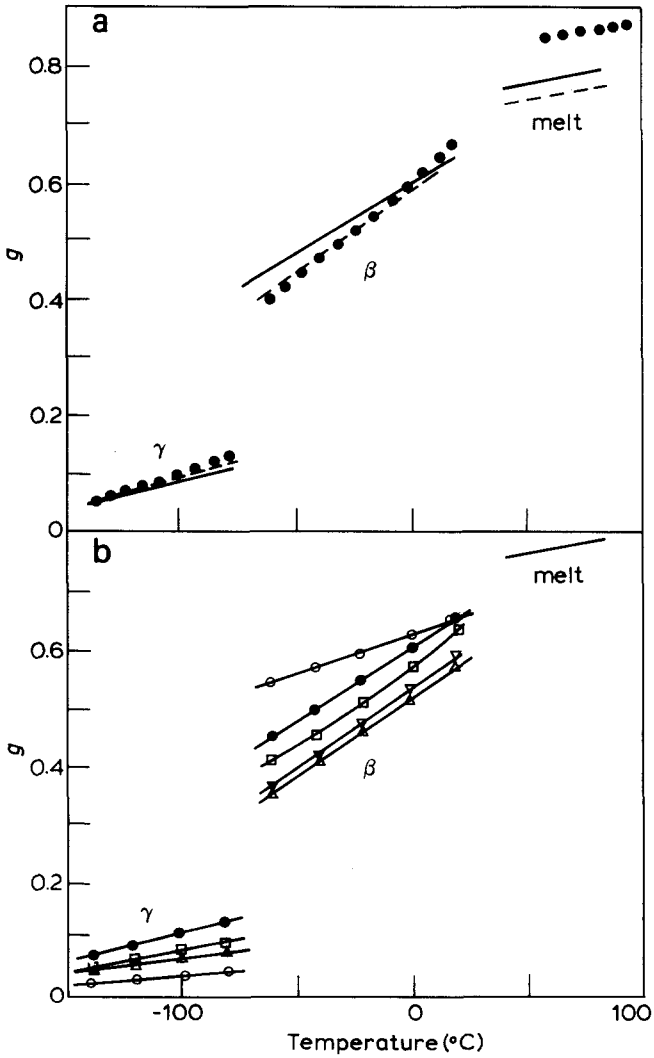

Figure 18 Kirkwood–Onsager dielectric correlation factor, g, for the amorphous fraction *versus* temperature in aliphatic polyesters (Boyd and Aylwin[43]). (a) Data for 6-6 (—), 6-10 (···), 5-7 (---) homopolymers. (b) Data for same copolyesters as in *Figure 15*

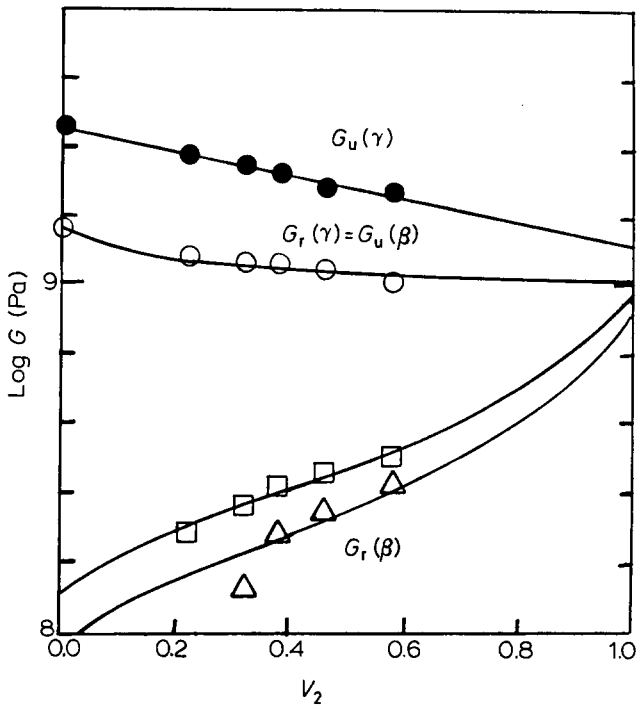

Figure 19 Relaxation strengths of the mechanical β and γ processes in aliphatic copolyesters *versus* crystallinity. The points are the relaxed and unrelaxed shear moduli of the two processes determined by phenonemological fitting of the data of *Figure 16*. The curves are calculated ones using the lamellar lower bound equations (Boyd[16]) and utilize an adjustable amorphous phase modulus (left-hand ordinate intercepts). The two values of G (β) (□), and (△) are at 250, 300 K respectively. Decrease in crystal modulus (right-hand ordinate intercepts) is due to assumed effect of thermal expansion not relaxation

chemical composition and the accompanying differing inherent strengths of the 6 and 6B units.

The relaxation strengths of the mechanical γ and β processes in the polyester copolymer series are displayed via the experimentally determined[44] limiting moduli vs. crystallinity in *Figure 19*. The curves were calculated from the lamellar lower bound equations[16] and use the amorphous phase shear modulus G_1 as an adjustable parameter. The β process is seen to be obviously assignable to the amorphous fraction. For the γ process, as was the case dielectrically, the relaxation can also be assigned to the amorphous phase when the variation of relaxation strength with diol composition as well as crystallinity is incorporated into the composite model for the relaxed γ process modulus. The lamellar lower bound gives a much better fit of the limiting moduli for the polyesters than the upper bound.

RELAXATIONS IN HIGH CRYSTALLINITY POLYMERS

General considerations

The discussion of these polymers is begun by showing some relaxation scans for several typical examples. For LPE there are a number of torsion pendulum studies as a function of crystallinity[4,46–50]. In *Figure 20* the data of Illers[51] that covers specimens of a very broad range of crystallinities, encompassing in fact the ranges of all the other studies is shown. For iPP the data of Passaglia and Martin[52] for samples of varying crystallinity is shown in *Figure 21*. Torsion pendulum scans for POM[53] are shown in *Figure 22*.

The most distinguishing feature of the relaxation behaviour of this class is the presence of an α relaxation. Because of the duality of phase assignment of relaxation strength depending on the kind of experiment (amorphous phase mechanically, crystal phase dielectrically or n.m.r.) it is important to demonstrate that in all of the experiments the crystal phase is involved. This can be accomplished by again invoking the 'strong' experiment of comparing relaxation in the semicrystalline solid with that in the melt[54,55]. At frequencies of $\approx$10 MHz the mechanical α processes are still in the vicinity of the melting region. Ultrasonic frequency measurements[55] of sound velocity and attenuation in LPE are shown in *Figure 23*. As the melting region is traversed in temperature there is a break in rate of decrease of sound velocity (proportional to the square-root of modulus) and a drop in the loss to zero. On cooling, the loss remains zero in the supercooled melt and reappears isothermally as crystallization starts and follows the same kinetics as the latter, showing that the presence of the crystal phase is required for the α process. Similar behaviour was found in iPP and POM. In lPE a similar result is obtained dielectrically[56].

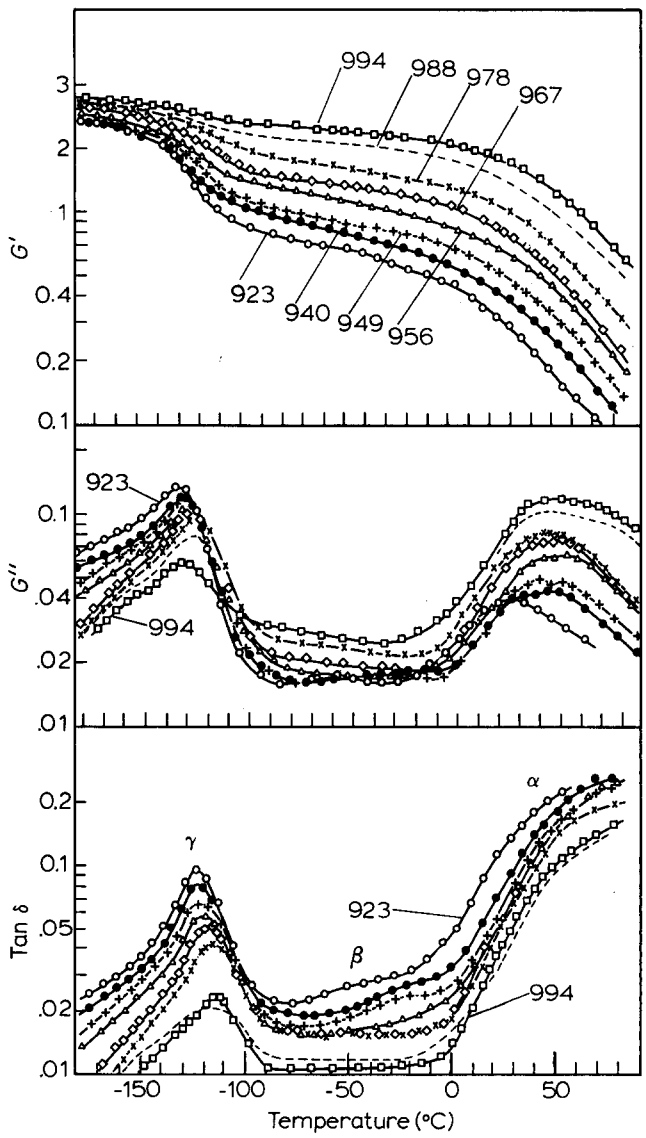

Figure 20 Dynamic shear response (G', G'' (GPA) and tan δ) *versus* temperature for LPE specimens of indicated densities (45–96% crystallinity) (torsion pendulum, Illers[51])

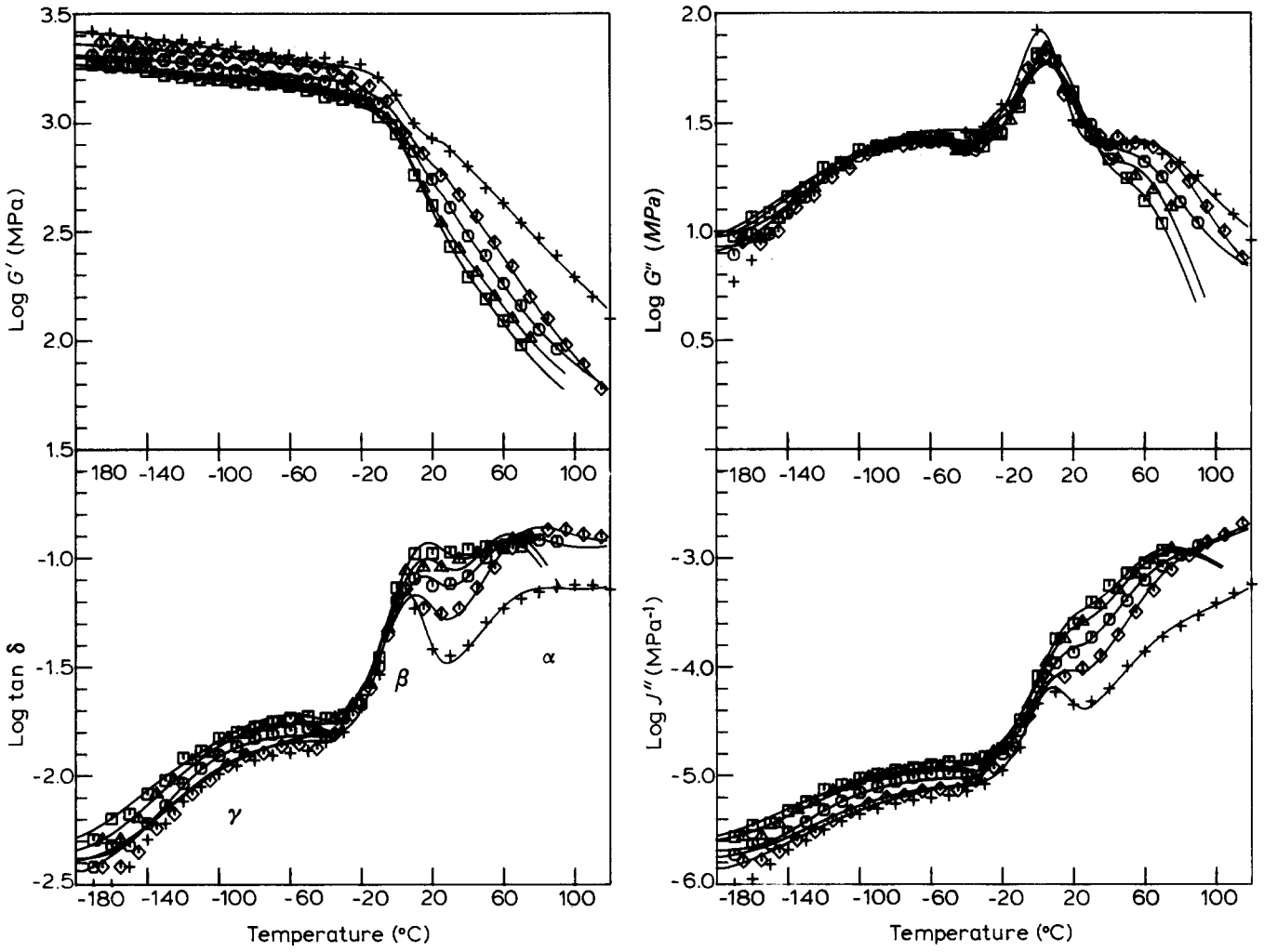

Figure 21 Dynamic shear response of isotactic polypropylenes of varying crystallinity *versus* temperature (torsion pendulum, ≈1 Hz, Passaglia and Marin[12]). (◇), 65%; (○), 56%; (△), 50%; (□), 45% crystallinity, first three specimens from annealing of quenched (45%) sample; (+), 68%, from isothermal crystallization). The curves are calculated from the mechanical Cole–Cole equation using parameters obtained from optimizing the fit to the data (Boyd[30])

Although PE is inherently not dielectrically active it can be decorated with a few C–Cl or C=O dipoles by chlorination or oxidation without seriously disturbing the morphology. The dielectric loss of a lPE specimen containing ≈1.7 C=O/1000 CH2 is shown in *Figure 24*. There is a normal progression of the isothermal frequency scan loss peaks with increasing temperature until the melting region is reached where the loss process suddenly disappears. As in the ultrasound measurements, reappearance of the loss from the supercooled melt was found to follow crystallization kinetics.

Having established a connection between the occurrence of the α relaxation and the presence of the crystal phase, the question of the assignment of the *mechanical* relaxation strengths of all three processes (α, β and γ) to the crystal and amorphous phases is now addressed. For the γ process in lPE, Gray and McCrum[4], from plots of relaxation strength and tan δ_{max} vs. crystallinity, concluded that the origin was largely amorphous but that there was a crystalline contribution as well. Later from data covering a wider crystallinity range Stehling and Mandelkern[47] argued for an entirely amorphous origin. Analysis[13] of the still wider crystallinity range data of Illers[51] showed rather clearly that the γ process does indeed disappear in 100% crystalline lPE. This analysis indicated that the α process also was to be assigned to the amorphous fraction. The latter conclusion, reached on unoriented bulk crystallized specimens, was in agreement with previous studies on oriented specimens[57,58]. There it was found that the direction of easiest deformation corresponded to shear of lamellar surfaces and hence amorphous layer deformation and not to deformations corresponding to crystallographic directions. More recently, a complete phenomenological analysis of the α, β and γ processes using the mechanical Cole–Cole equation has been carried out[29] for Illers' data (*Figure 25*). The result of this analysis with respect to relaxation strengths is shown in the form of limiting moduli vs. crystallinity in *Figure 26*. It seems clear that all three mechanical processes are to be assigned to the amorphous phase. Reexamining *Figure 20* and comparing the crystallinity dependence of log G''_{max} with that of log tan δ_{max} a good example regarding the comments in the section on morphological assignment is seen. The variation of log G''_{max} (in this lower bound-like material)is not a good indicator of assignment. For the γ process it varies little with crystallinity over most of the range and for the α and β processes it varies in the opposite direction of relaxation strength. For the tan δ_{max} however the variation with crystallinity corresponds with the variation of relaxation strength for all three processes. Although not displayed, J''_{max} correlates with amorphous origin for all three

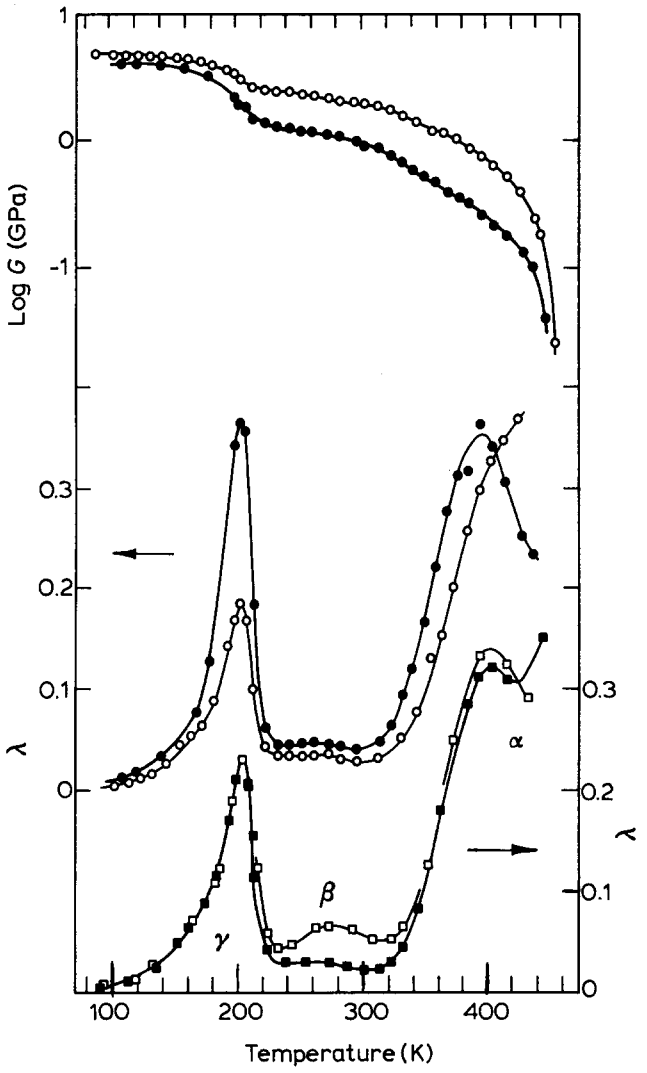

Figure 22 Shear modulus and log decrement of POM (torsion pendulum, McCrum[53]), specimens of two crystallinities ((○), 76%; (●), 59%) are shown (left-hand ordinate scale). Also shown, are the log decrements (and plotted on right-hand ordinate scale) of a specimen measured immediately after cooling from the *solid* at 157°C (□) and the same sample measured after storage at room temperature (■)

processes. This is important because in fitting the limiting moduli variation with crystallinity it was concluded that lower bound-like behaviour was experienced. Therefore this behaviour of J''_{max} is necessary for consistency (*Figure 1*) and is additional evidence for lower bound-like behaviour.

Unfortunately, for other polymers there is not much data available for making assessments like those above for lPE. However, phenomenological analysis similar to that accomplished for lPE has also been carried out[30] on the data of Passaglia and Martin[52] for iPP (see *Figure 21*). The resulting relaxation strengths are displayed in *Figure 27*. Five specimens were studied. One of them was a quenched sample and three had higher crystallinity levels produced by annealing of the former. The fifth one (with the highest crystallinity) was prepared by isothermal crystallization. The curves in *Figure 27* were calculated from the lamellar lower bound equations[16] using estimated elastic constants for the crystal phase. Again, amorphous phase origin of all three processes can be accommodated by the relaxation strength variation with crystallinity. For the γ process, the relaxation strength is so small that variation of the unrelaxed modulus with crystallinity is essentially as great as that of the relaxed modulus. Thus the relaxation strength variation is not very definitive and only indicates that amorphous origin is consistent with the strengths. For the β and α processes the conclusion with respect to amorphous origin is more definitive. It is of interest to note that for the β and α processes the relaxed moduli of four of the specimens appear to vary smoothly with crystallinity. However the fifth, the isothermally crystallized one, has significantly higher values. Thus the specimen moduli in these relaxation regions do not seem to be a unique function of crystallinity, the isothermally produced specimen having a higher modulus than an annealed specimen of similar crystallinity. This may be related to the observation that X-ray diffraction patterns of quenched iPP specimens

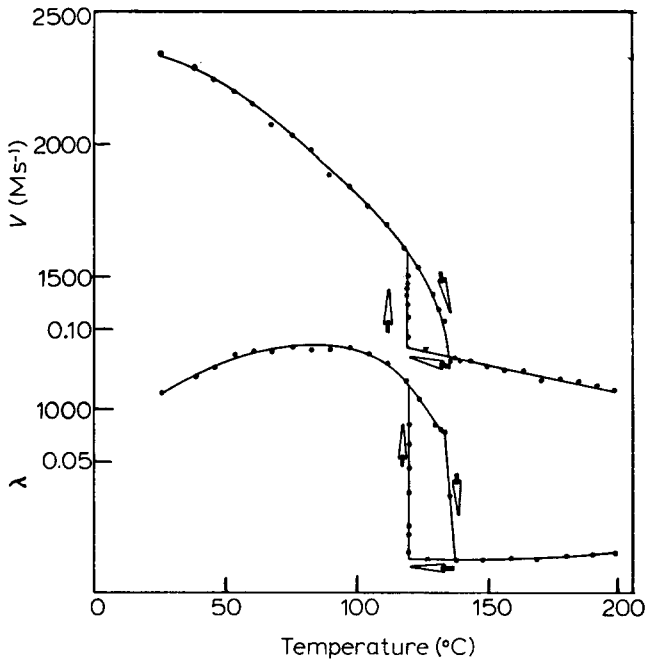

Figure 23 LPE α relaxation, sound velocity and log decrement *versus* temperature through the melting region (9 MHz ultrasonic waves, Boyd and Biliyar[23])

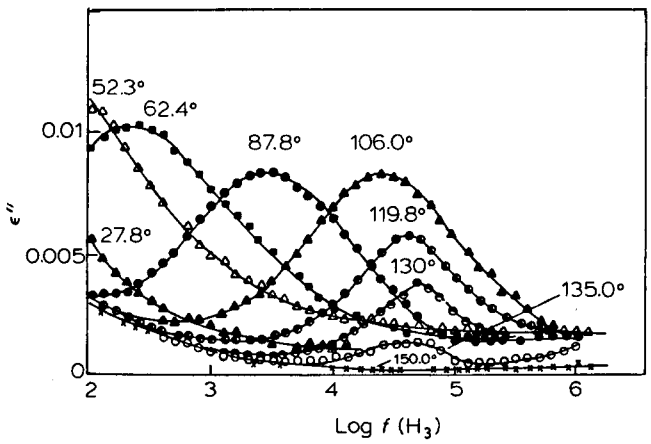

Figure 24 LPE α relaxation, dielectric loss plotted *versus* log frequency at several temperatures through the melting region (lightly oxidized specimen, 1.6°C=0/1000 methylenes, Ashcraft and Boyd[56])

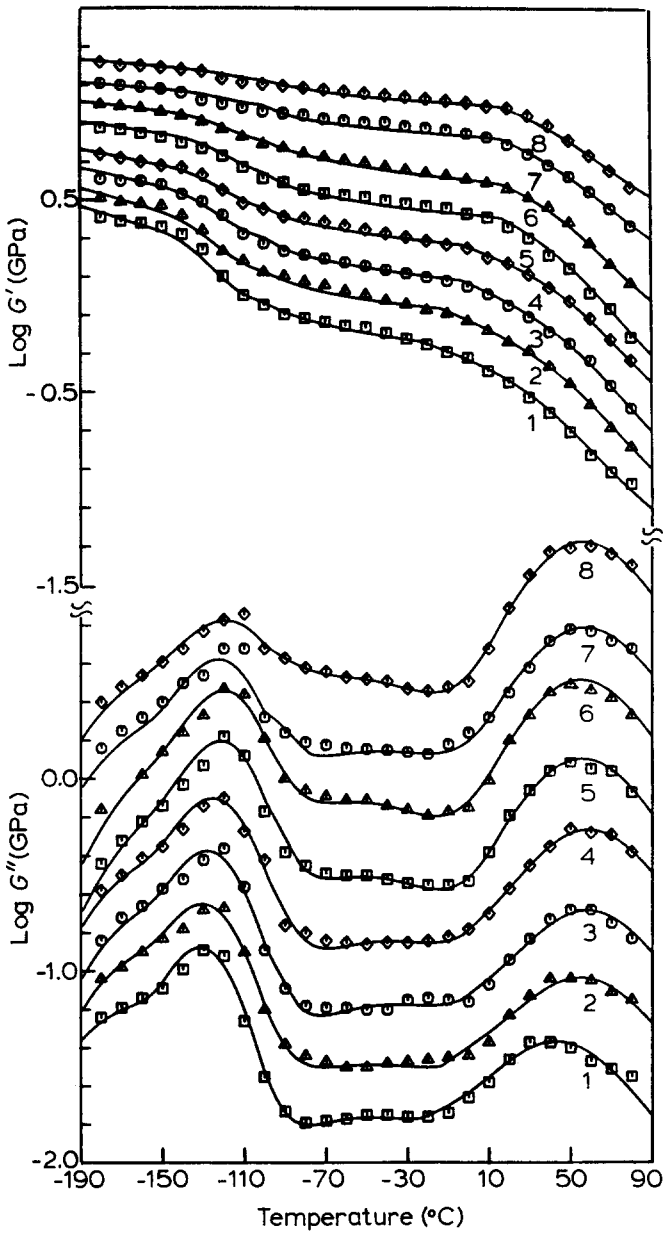

Figure 25 Phenomemological fits of the complex shear modulus of LPE. Points are representative of Illers data[51], curves were calculated from the Cole–Cole mechanical equation using parameters obtained by optimizing data fit (Boyd[29]). Each log G' curve is displaced upward 0.1 unit with respect to preceeding one for clarity in plotting, each log G'' by 0.3

show considerable deterioration in sharpness but on annealing the pattern sharpens considerably (see, for example, ref. 59). This has often been taken as evidence for disordered crystals (i.e. a 'smectic phase') in quenched specimens. Thus it may be that the two-phase model of well-developed crystals plus the amorphous fraction may be inadequate here. The situation does seem to stand in contrast to lPE where modulus variation with crystallinity seems to be remarkably independent of how the crystallinity level is produced. It is interesting to compare the variations of G'', J'' and tan δ with crystallinity in the context of morphological assignment. It can be seen in *Figure 21* that G'' varies little with crystallinity in the γ and β regions and varies opposite to relaxation strength in the α region and thus is not a good indicator of phase origin. On the other hand J'' correlates with amorphous origin for all three processes in agreement with relaxation strength. The J'' and relaxation strength behaviour taken together is an indicator of lower bound-like behaviour. In other words, if lower bound-like equations are thought to fit the limiting moduli and they indicate amorphous origin, then J'' should also correlate as an amorphous process. On the other hand G'' should be expected (*Figure 1*) to be insensitive to crystallinity or vary in the opposite direction to relaxation strength. Such is the case here for iPP. The behaviour of tan δ_{max} is a little more complicated. For the γ and β processes it correlates as expected as an amorphous process but for the α process the three annealed specimens vary in the opposite direction. This appears to be the result of the combined effects of the displacement of the α peak to higher temperature with increasing crystallinity (no doubt due to increasing crystal thickness, see below for PE) and the decrease of the relaxed and unrelaxed α moduli with increasing temperature. That is, the higher crystallinity annealed specimens have lower values of G' appearing in the denominator of tan δ and this is due not to relaxation but, rather, to decreased limiting moduli as the temperature region of the relaxation increases. The consequences of the variation of peak *location* with crystallinity were not incorporated into the simplified calculations underlying *Figure 1*. The data of Flocke[60] on the shear modulus of polypropylenes

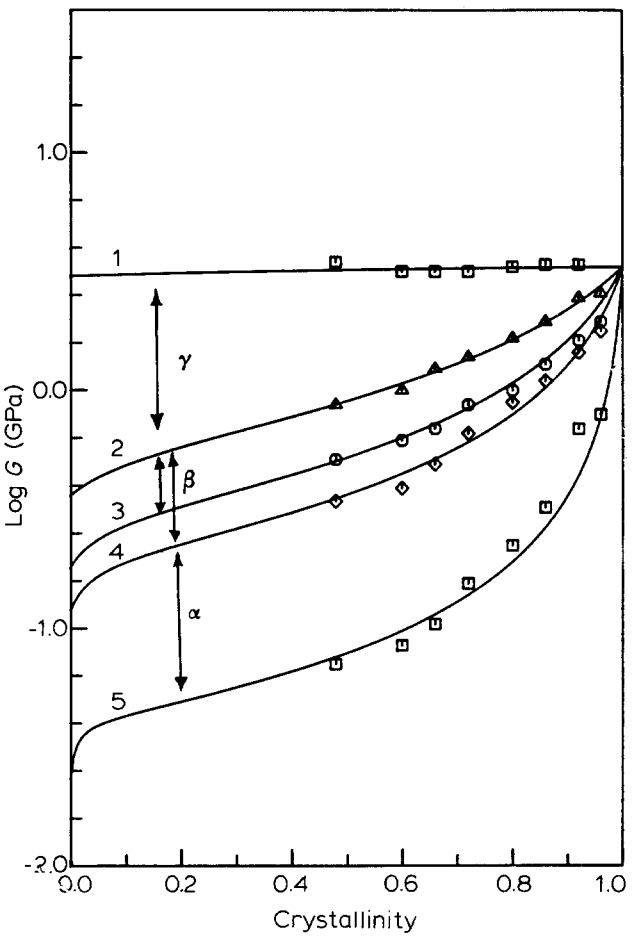

Figure 26 Relaxation strength *versus* crystallinity in LPE (Boyd[29]). Relaxed and unrelaxed shear moduli for the α, β and γ processes. Points are from phenonemological fits (*Figure 25*), curves are calculated from lamellar lower bound equations using adjustable amorphous phase shear modulus. Two curves (3,4) are shown for the relaxed β process modulus, one at 175 K, another at 300 K. Curves 1, 2 are unrelaxed, relaxed γ moduli, 5 is relaxed α process

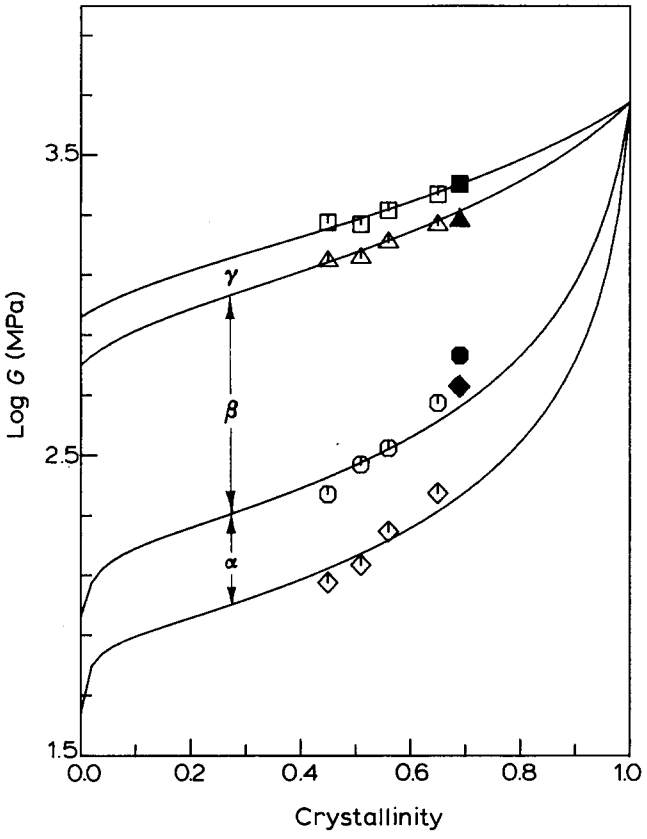

Figure 27 Relaxation strength versus crystallinity in IPP (Boyd[30]). Relaxed and unrelaxed shear moduli for the α, β and γ processes. Points are from phenonemological fits (*Figure 21*), curves are calculated from lamellar lower bound equation using adjustable amorphous phase shear modulus. (□), (△), (○), (◇): quenched and annealed specimens, (■), (▲), (●), (◆): a isothermally crystallized sample

of varying tacticity and hence crystallinity also confirm that the mechanical α process is to be assigned to the amorphous phase. To summarize, although there is less data available with respect to crystallinity variation of moduli, iPP appears to behave in a manner similar to lPE in that the mechanical relaxation processes are assigned to the amorphous fraction and in that the mechanical behaviour is lower bound-like. There does not seem to be suitable data available for other high crystallinity polymers for making similar analyses.

The α process

A case has been made for regarding the mechanical α, β and γ processes in lPE as assignable to the amorphous phase. More detailed discussion of the characteristics of the individual processes in this polymer including the phase assignment in dielectric and n.m.r. measurements is now taken up. In dipole decorated PE the dielectric constants of the two phases are very similar since the material is only very slightly polar. This means that the composite behaviour is immaterial and relaxation strength should be directly proportional to a phase volume fraction and the dipole concentration in the phase. Dielectric relaxation strength plotted vs. crystallinity shows[56] that the process is to be assigned to the crystal phase. An obvious auxillary conclusion is that the carbonyl groups are incorporated into the crystals. The relaxation strength does not follow a straight-line relation vs. crystallinity and this is attributed to some selective partitioning of carbonyl groups away from the crystals. However the strength of the process is great enough to indicate that all crystal dipoles participate in relaxation and that it does not indicate a mechanism involving a few chains associated with crystal defects. Another indication that the process originates directly in the crystals is derived from the anisotropy or relaxation in oriented specimens. Since carbonyl dipole direction is normal to the chain direction in the planar zig-zag, a relaxation originating in the crystal should be intense in the direction normal to the *c* axes and of zero strength parallel to this direction. The α relaxation in specimens cut from rods oriented by solid-state extrusion shows just this kind of anisotropy[61] (*Figure 28*). The degree of orientation produced in the amorphous fraction is far too small to produce this degree of anisotropy. The dielectric α process is found to be rather narrow in the frequency domain with Cole–Cole width parameters in the range 0.7–0.8[56]. The activation energy for the central relaxation time is 100–120 kJ mole^{-1}. For the mechanical α process the time temperature behaviour has been established by creep measurements[62,63], frequency domain dynamic measurements[62] and by phenomenological analysis of the isoch-

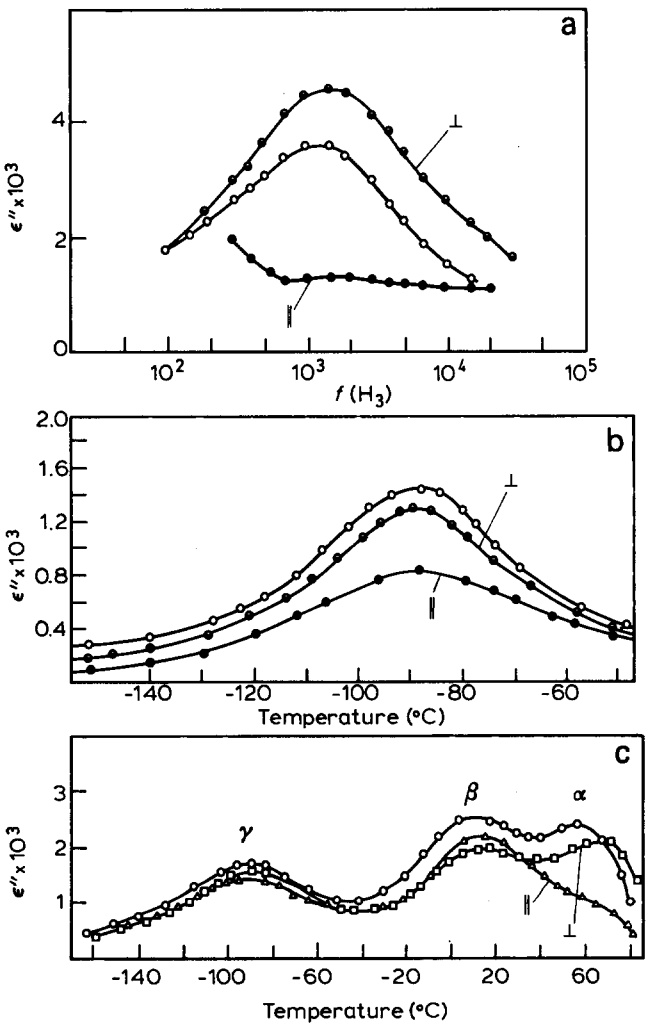

Figure 28 Anisotropy of dielectric relaxation in oriented PE. (a) relaxation of LPE at 80°C, ∥ and ⊥ refer to direction of dielectric measurement with respect to extrusion direction in oriented rod (○): unoriented in all three sets. (b) curves for γ process in LPE (10 kHz). (c) curves for isochronal scans through all three processes in BPE (lightly oxidized samples, 10 kHz, Boyd and Yemni[61])

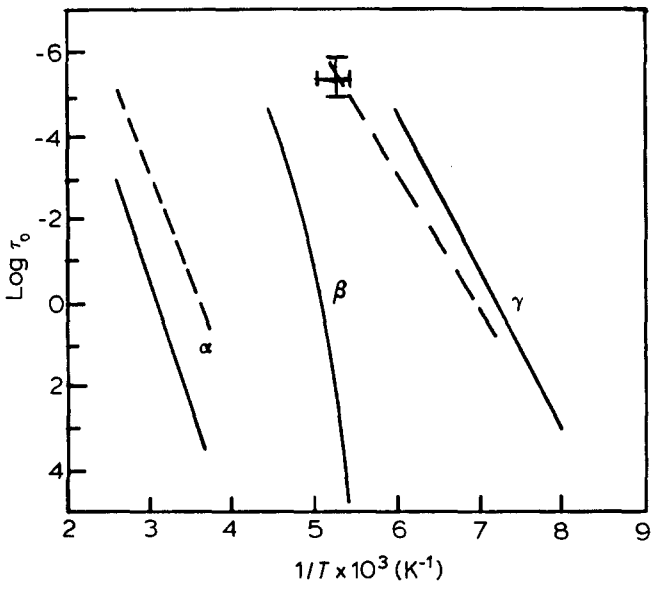

Figure 29 Loss map (log τ_0, Cole–Cole central relaxation time, *versus* $1/T$) for LPE. Solid and dashed curves are mechanical and dielectric results respectively on similar specimens (Boyd[29]). Cross is n.m.r. result (Bergmann[81])

ronal torsion pendulum scans[29]. The mechanical process is complex[62,63], showing evidence for an additional partially resolved process above the temperature limit of Illers' data (*Figure 20*). The two processes were designated α, α′ by McCrum and Morris[63], α I, α II by Nakayasu *et al.*[62] The Cole–Cole mechanical equation fits[29] of torsion pendulum scans (*Figure 25*) also fit the creep and dynamic data for the α (or α I) process. The parameters from this fitting (as well as the data itself) show the mechanical α (not including α′ or α II) process to be considerably broader than the dielectric one. The mechanical Cole–Cole $\bar{\alpha}$ width parameter is ≈0.4 (cf. 0.7–0.8 dielectrically). The central relaxation time mechanically lies consistently at longer time isothermally than dielectrically. However the activation energies for the mechanical and dielectric central relaxation times are quite similar[56,62,63]. A comparison of log τ_0 is made via a loss map in *Figure 29*.

An interesting feature of the α process is that the location depends on the crystal lamellar thickness. This is true both dielectrically and mechanically and the observation holds for both bulk crystallized specimens and for single crystal mats. For the latter, the mechanical α process does not show evidence for complex structure (α,α′) and appears to be a single (broad) process[64–67]. Another important observation is that the process can be observed dielectrically in even-numbered paraffins that contain small amounts of dissolved aliphatic ketones of one less carbon atom[68]. However the process is not observed mechanically in well purified paraffin crystals[69,70] (where no amorphous fraction is present, in agreement with the assignment of the mechanical relaxation strength to the amorphous phase). In *Figure 30* T_{max} (1 kHz) values measured dielectrically[56] are shown for a wide variety of specimens. Mechanical measurements (E'') at 110 Hz are also shown*. These are compared to the dielectric results shifted to the same frequency. In addition, torsion pendulum results[64] at 1 Hz on single crystals are shown and compared with frequency extrapolated dielectric results. The mechanical single crystal results correlate with the bulk specimen mechanical α process (not the α′). Dielectrically the data for the ketone-containing paraffins correlates well with the single crystal and bulk specimen data. The shorter relaxation times for the dielectric process compared to the mechanical one are again apparent (*Figure 30*), now as lower (isochronal) T_{max} values (cf. isothermal comparison above, *Figure 29*).

N.m.r. studies have a great deal to say about the α process also. In their definitive study of broad-line proton resonance in PE, Olf and Peterlin[71] derived expressions for the second moment for a number of models for the α and γ processes and compared them with their measured values. For the α process the models included defect motion within the crystal, various representations of restricted rotational oscillation abut the *c* axis as well as the 180° rotational jump accompanied by translation by one methylene group along *c* that leaves the chain in crystallographic register. Of these models only the latter one (180° rotation–C/2 translation with all crystal chains participating) was in accord with the changes in the second moment through the relaxation measured at various angles to the *c* axis in an oriented single crystal mat (see *Figure 31* for the experimental second moment

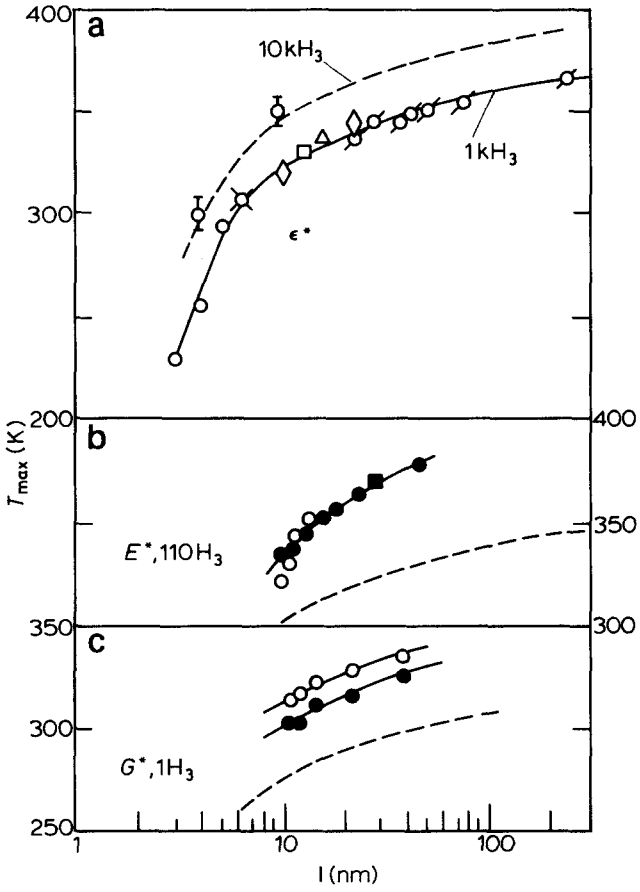

Figure 30 α process location (T_{max} isochronal) *versus* crystal thickness in PE and paraffins. (a) Dielectric data (1 kHz). Oxidized LPE; (⊠), oxidized BPE; (◇), Cl LPE; (□), single XL LPE; (○), paraffins; see Ashcraft and Boyd[56], for sources of data). The upper curve (– – –) is the dielectric solid curve shifted to 10 kHz for comparison with the two points (Φ) which are n.m.r. results on a paraffin (Olf and Peterlin[75]) and a single crystal mat (Olf and Peterlin[72]). (b) Results from complex tensile modulus (E'') at 110 Hz (Takayanagi[65]) ((○): isothermally grown single XLs; (●): annealed single XLs, (■), bulk specimen (– – –) dielectric curve shifted to 110 Hz). (c) Results from shear modulus of annealed single XLs (torsion pendulum, 1 Hz, Sinnott[64]). ((○) tan δ_{max}, (●) from G''_{max}). (The lower curve (– – –) is the dielectric curve shifted to 1 Hz)

* Note added in proof: Further results on α-peak location and crystal thickness have recently been reported[112].

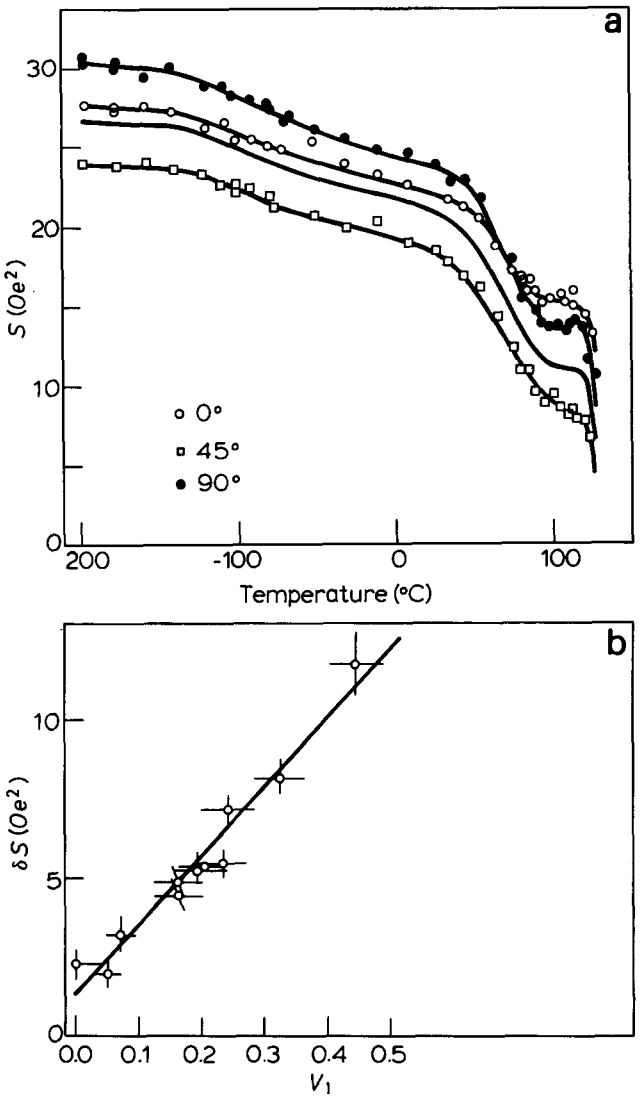

Figure 31 N.m.r. results on PE. (a) Second moment of PE single crystal mat *versus* temperature; three orientations and powder average (curve without points) are shown. (b) Total decrease in the second moment from −196°C–20°C as a function of the amorphous fraction. Results are for a variety of samples including extended chain and nitric acid etched (Olf and Peterlin[72])

temperature scan)[72]. The success of the Olf–Peterlin analysis depended on experimentally locating the high temperature plateau or relaxed value of the α process second moment. Because of the relatively high n.m.r. frequency and the temperature scan method required, the plateau is not observable in bulk crystallized specimens. However in the very thin single crystals selected, the α relaxation occurs at sufficiently low temperature compared to the melting point to present a plateau in temperature scans. The location of the n.m.r. process correlates with that of the dielectric one and thus is somewhat faster than the mechanical one (see *Figure 30*). Analysis of the α process proton broad-line resonance in bulk crystallized LPE was necessarily less conclusive[73]. An interesting experiment carried out by Opella and Waugh[74] using 'two-dimensional' ^{13}C n.m.r. leads to a rather unequivocal conclusion that the 180° rotation–C/2 translation is indeed the motion taking place. An α relaxation has also been found in the broad-line spectrum of paraffins[75] (see *Figure 30*).

To recapitulate the behaviour of the α process in PE, there is strong evidence that the dielectric and n.m.r. methods measure processes directly associated with the crystals and result from reorientational motions within them. In contrast, the mechanically active α process, although it requires the presence of the crystal phase, has its relaxation strength assigned to the amorphous component and involves softening or deformation of the latter. Although the activation energies are similar, the relaxation times are longer mechanically than dielectrically (or by n.m.r.) and the mechanical process is much broader in relaxation times than the dielectric process. The relaxation times for all the processes depend on crystal or lamellar thickness.

For other polymers there is less quantitative information concerning the relaxation parameters for the α process. However from creep and dynamic compliance Gray[76] has established the activation energy for this process in POM and McCrum[77] has established a value from creep measurements for iPP. It has been found possible to construct master creep curves using time–temperature superposition. This implies that for the α process the width of the relaxation time distribution is at least to a fair approximation independent of temperature. It is absolutely essential in constructing these curves to realize that the unrelaxed and relaxed compliances are quite temperature dependent. Major vertical shifts as well as horizontal ones are thus required in the reduction to a master curve. Otherwise entirely erroneous values for the activation parameters will result.

The β process

The β process in lPE is not a prominent feature in the relaxation spectrum (i.e. G''_{max} or tan δ_{max} relative to those of the other peaks). However the data to (*Figure 20*) show its presence*. It is of course of considerable interest to examine the reasons for the variations in the relative prominence of β relaxations among various crystalline polymers. As a start, this is conveniently done on a phenomenological basis. The analysis[29] underling the fits in *Figure 25* permits comparison of the mechanical relaxation parameters of lPE with those of other polymers that have been similarly analysed. Relaxation strengths expressed as the limiting moduli of a 50% crystalline polymer are displayed in *Table 2*. These limiting moduli were all determined by fitting the mechanical version of the Cole–Cole equation to torsion pendulum shear modulus data. From examination of *Table 2* it may be concluded that lPE does have the lowest β process relaxation strength and this contributes of course to a relatively small peak height in G''. It is interesting to note that the combined strength of the γ and β processes for lPE is quite comparable to those of the other polymers listed. This means that the lower strength of the β relaxation in lPE is not due to a lesser degree of softening through the β process but rather to a stronger γ process that results in a lower unrelaxed modulus for the β relaxation. It is seen that bPE also has a strong γ process but that it also has a rather low relaxed β modulus to that the β strength is quite high. In iPP the relative prominence of the β peak is enhanced due to both the γ and α processes being weaker than in lPE. The β process is quite broad in the frequency domain for lPE[29] but apparently no more so than for bPE and iPP[30]. The temperature dependence of τ_0 is a contributing factor to the isochronal loss peak

* Note added in proof: There now appears to be agreement on this point. A recent paper by Mandelkern and co-workers[112] reports β relaxations in lPE.

Table 2 Mechanical relaxation strengths [a], Δ

Polymer [b]	log G_U	γ (or β) subglass log G_R	Δ	log G_R	β (or α_a) $S_R \times 10^3$ [c]	Δ	α log G_R	Δ
lPE	0.50	−0.05	0.55	−0.45	−4.0	0.40	−1.10	0.65
bPE	0.40	0.00	0.40	−0.86	−13.0	0.86	−1.30	0.44
iPP	0.27	0.15	0.12	−0.55	−5.0	0.70	−0.88	0.33
PET	0.23	0.04	0.19	−0.59	−2.0	0.63	–	
CO 6–6/6B–6	0.30	0.04	0.26	−0.65	−3.0	0.69	–	
IPS	–	0.10	–	−1.10	−2.0	1.20	–	

[a] Expressed as log G_U–log G_R (G_U G_R in GPa) of a 50% crystalline specimen. Where exp. crystallinity range does not cover 50%, lamellar lower bound equations were used to extrapolate to 50%. Mechanical Cole–Cole equation was used to fit data and determine limiting moduli

[b] lPE=linear polyethylene, exp. data, (ref 51); bPE=branched polyethylene, (ref 60); iPP=isotactic polypropylene, (ref 52); PET=polyethyleneteraphthalate, (ref 19); Co 6–6/6B–6=aliphatic copolyesters (see text), (ref 30); iPS=isotactic polystyrene, (ref 32).

[c] The relaxed beta (α_a) moduli are very temperature dependent, S_R is the temperature coefficient of log G_R the latter is listed at 300 K for all polymers but PET (400 K) and iPS (400 K)

shape for lPE. The isochronal sharpness is inversely proportional to the average activation energy[1]. In lPE the β process occurs at relatively low temperature and has a relatively low activation energy. Although this does not affect peak height it does lead to an especially broad isochronal peak and therefore to poor resolution. Finally it is important to realize that although thermal treatments (quenching) can be effective in producing a larger amorphous fraction the *relative* prominence of the α, β and γ peaks is changed but little as *all three* correlate mechanically as amorphous processes.

As is apparent in *Table 2* the relaxed modulus for the β process is quite high for all of the polymers and it is also quite temperature dependent, decreasing markedly with increasing temperature. As previously commented this must be a reflection of the effect of the crystals in immobilizing amorphous segmental reorientation. Unfortunately, in the high crystallinity class there does not yet seem to be appropriate dielectric data available for assessing the β process dipole correlation factor and the effect of immobilization by the crystal phase on it (see PET and aliphatic polyesters).

N.m.r. measurements (like other relaxation methods) tend to sample certain kinds of molecular motions but within these types the results are indiscriminate as to detail[78,79]. In the case of the α process, resolution of the second moment contribution was possible in temperature scans on single crystals (see above). In general, however, analysis of line-shapes from isothermal broad-line or pulse techniques into contributions from multiple processes is, like other relaxation methods, difficult. One of the difficulties in resolving the n.m.r. line-shapes into components from the various processes is that the fundamental line-shapes of the components are not necessarily known. Resolution of the broad-line proton spectrum into a broad component from the crystals with the rest arising from the amorphous fraction is fairly straightforward. By using assumed empirical analytical representations for the line-shapes Bergmann[80] has further resolved the amorphous contribution into medium and narrow components. The medium component was associated with the γ relaxation and the narrow one with the β process. In a later refinement of the resolution process, the identification of the medium and narrow components was changed to have them both correspond to the γ process[81]. This reassignment was based on associating the beginning of the narrowing of the n.m.r. components with measures by other techniques of the centres of the relaxation processes. However, if the *centre* of narrowing of the n.m.r. medium component (at ≈190–200 K) is compared to the *centre* of the dielectric γ relaxation (T_{max} at 10–100 kHz, the n.m.r. frequency) close correspondence between the two processes is observed (*Figure 29*). The centre of narrowing of the narrow process cannot be located with certainty but lies at higher temperature than the dielectric γ process at the same frequency and is consistent with the temperature range of a broad β process. Regardless of the validity of the resolution of the amorphous component relaxation into contributions from various processes all the n.m.r. studies agree that, in lPE for example, molecular motion in the amorphous fraction is restricted, becomes less so with increasing temperature, but remains restricted in the solid compared to a melt or an amorphous polymer above the glass transition.

As in other crystalline polymers (*Figure 7*) the β relaxation in lPE is sensitive to the plasticizing action of diluents[82,83]. In *Figure 32* torsion pendulum shear modulus and loss data[83] for lPE containing 11 wt% carbon tetrachloride is compared to that for a dry sample. The plasticized sample now has a prominent β G'' peak at ≈ −80°C compared to a broad one at ≈ −50°C in the dry sample. Examination of the G' curves shows that a major contributor to the increase in peak height is a decrease in the relaxed modulus of the β process and hence increased relaxation strength. It is evident then that the diluent is effective in removing constraints on the amorphous segments and in making more configurations available to reorientation. It is also probable that the β process is narrower in the time domain but no phenomenological analysis has been carried out to confirm this. Another experiment that has been used to produce a more intense mechanical β loss peak in lPE[50] and POM as well[53], is to rapidly quench the specimen to low temperature, not from the melt (to produce a larger amorphous fraction), but rather from high temperature in the solid (to freeze in greater free volume in the amorphous fraction). Such specimens show a much more pronounced β peak (*Figure 22*).

As in other crystalline polymers the β process in PE can be traced to the completely amorphous state by eliminating the crystallinity through copolymerization[84–90]. Most of the copolymer studies have used high pressure polymerization and hence have made a connection be-

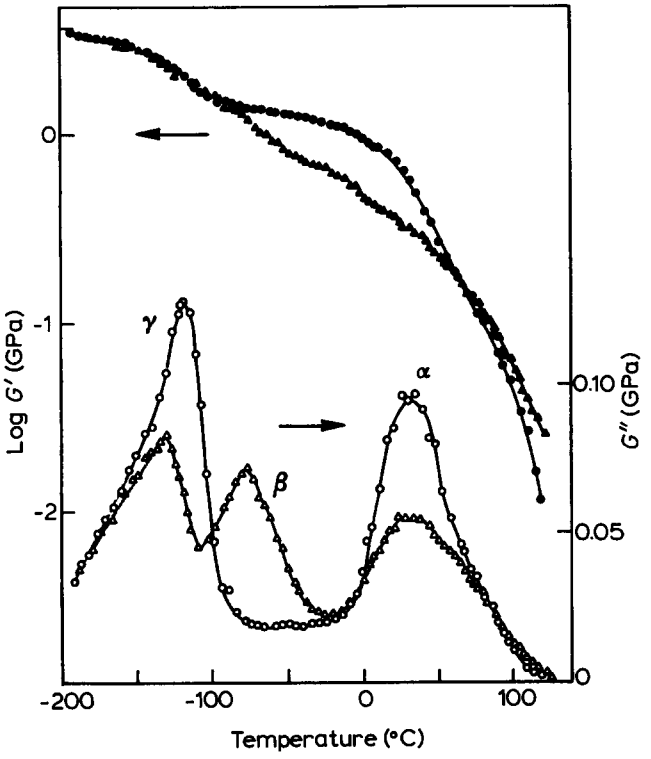

Figure 32 Complex shear modulus of LPE swollen with carbon tetrachloride (11 wt%) ((△) and (▲)) compared to unswollen material ((○) and (●)) (Arai and Kuriyama[83])

tween the glass–rubber relaxation in completely amorphous copolymers and the β relaxation in bPE rather than lPE. However, it is to be presumed that the β relaxation in bPE is analogous to the observed β process in lPE and that the former polymer is itself simply to be regarded as a copolymer of the latter. That is, for our purposes, bPE is a copolymer involving mostly ethylenic units and a few per cent of 1-alkenes (predominately 1-hexene, giving rise to C_4 branches). It is unlikely that the long chain branches have a major effect on relaxation. The results of the seminal experiments of Schmieder and Wolf[84] on the chlorination of bPE and of Nielsen[85] on bPE/PVAc copolymers are recapitulated in *Figure 33* and *Figure 34* respectively. The results of both experiments are very similar. As the mole per cent of comonomer increases the α peak is displaced to lower temperature, no doubt due to a decrease in lamellar thickness. Accompanying this is a large increase in the strength of the β relaxation. For both systems, at the highest comonomer content shown there is only a slight vestige of crystallinity left and the α process essentially has disappeared in agreement with the premise that the presence of the crystal phase is required (upturns or peaks in the loss near the highest temperatures are probably artifacts due to melting or final softening). It is obvious that the β relaxations have grown into typical amorphous polymer glass–rubber relaxations. In contrast, in the case of the chlorinated bPE, the γ relaxation is little disturbed by this degree of chlorination. Although the data of Nielsen do not include the γ region it is apparent from the behaviour of the unrelaxed β process modulus and the findings of Reding *et al.*[87] that T_{max} for the γ process is insensitive to composition that the γ process in bPE/PVAc copolymers is also not very sensitive to the presence or degree of crystallinity (beyond relaxation strength change with chemical composition (cf. the behaviour of aliphatic polyester copolymers). A recent statement by Popli and Mandelkern[91] that crystallinity is necessary for the occurrence of a β relaxation is clearly not supported by data such as that in *Figures 33* or *34*. Although the β process relaxation parameters (especially the broadness) may change rather abruptly with the onset of crystallinity (cf. aliphatic polyesters) the process itself clearly is traced continuously from crystalline to non-crystalline specimens. Earnest and MacKnight[86] have studied a copolymer system that does lead to direct lPE comparison, they studied mechanical relaxation in *cis* polypentenamer (a low T_g elastomer) hydrogenated to various degrees (including all the way to lPE). They found that the transition to lPE-like behaviour, with a broad β

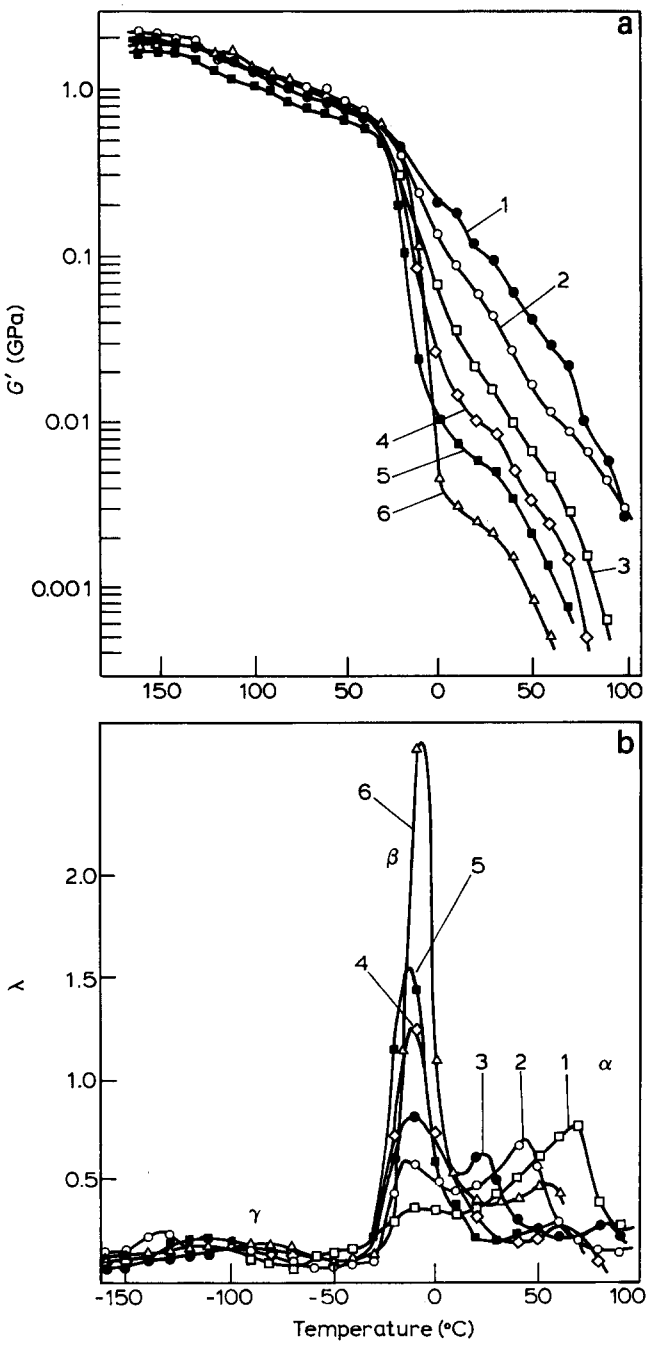

Figure 33 Effect of chlorination on the shear modulus and log decrement of BPE (curves 1–6 are 0, 5.8, 10.4, 14.7, 19.3, 28.2 wt% CL respectively). (Torsion pendulum, ≈1 Hz, Schmieder and Wolf[84])

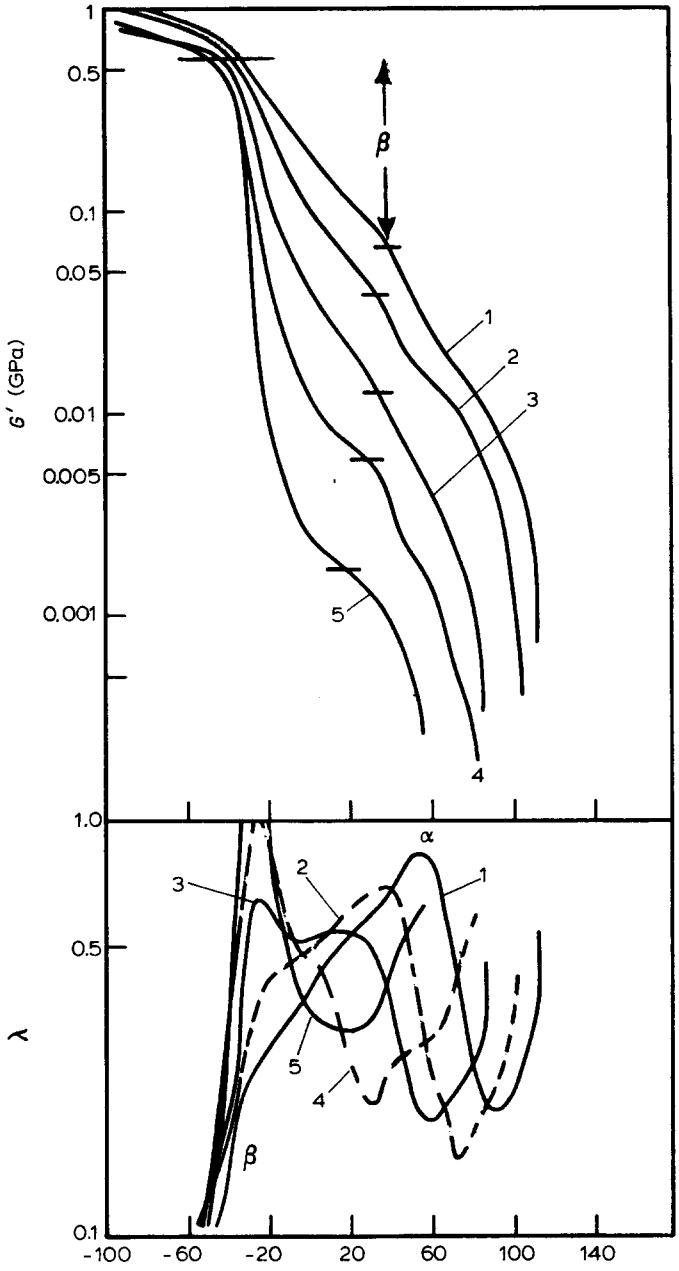

Figure 34 Effect of copolymerization with vinyl α acetate on the shear modulus and log decrement of BPE in β and α regions (curves 1–5 are 0.0, 3.0, 7.0, 10.6, 20.0 mol% vinyl acetate respectively). (Torsion pendulum, ≈1 Hz, Nielsen[85]). Approximate limiting moduli for β relaxation are marked

relaxation and with the presence of an α relaxation, occurred rather suddenly along with the onset of crystallinity as degree of hydrogenation increased. This is further indication of the profound effect of the crystals in influencing the amorphous phase glass–rubber relaxation and also provides confirmation of the α process requiring the presence of the crystal phase even though its relaxation strength is associated with the amorphous fraction.

Heat capacity is subject to relaxation effects and has been extensively discussed in relation to the relaxations in crystalline polymers such as PE. Heat capacity results[92] for a representative lPE sample are shown in *Figure 35*. In order to be able to resolve relaxation regions from the general contributions from internal and lattice vibrations it is convenient to construct a baseline based on 100% crystalline lPE. Several such baselines have been constructed by extrapolation of experimental results versus crystallinity and agree reasonably well[93,94]. A 'difference plot' of the experimental heat capacity, with the extrapolated 100% crystalline polymer baseline[93] subtracted, is shown in *Figure 35*. Qualitatively, the difference plot shows virtually the same behaviour as the isochronal shear modulus in the same systems. That is, there are (poorly resolved) increases in heat capacity in each of the three temperature regions corresponding to relaxation processes measured mechanically at low frequency. Beatty and Karasz[95] have suggested that there is a heat capacity increase reflective of a relaxation process only in the γ temperature region (130–190 K). However their conclusion resulted from using a baseline from a single non-representative sample. The experimental data (theirs and others) when differenced against more representative base lines (*Figure 35*) do not support this conclusion.

The time dependence of volume relaxation in the β region in lPE has been studied by Davis and Eby[96]. They found that it has the WLF behaviour characteristic of a glass–rubber relaxation. The dependence of thermal expansion data on temperature and crystallinity in lPE has been analysed by Boyer[97]. Resolution of change in thermal expansion through the β region into two contributions was advocated. These were attributed to the glass–rubber relaxations in constrained and unconstrained amorphous regions. Given the inherent broadness of the relaxation this resolution necessarily has considerable arbitrary character about it.

Completely amorphous lPE, produced by rapid quenching of very thin specimens, has been the subject of relaxation study[98,99]. The relaxation response of an amorphous specimen supported on a glass braid was measured with a torsion pendulum. The initial scan on warming the quenched material showed four relaxation peaks. The lowest temperature one (at 150 K) corresponded to the γ process. A peak at 190 K was

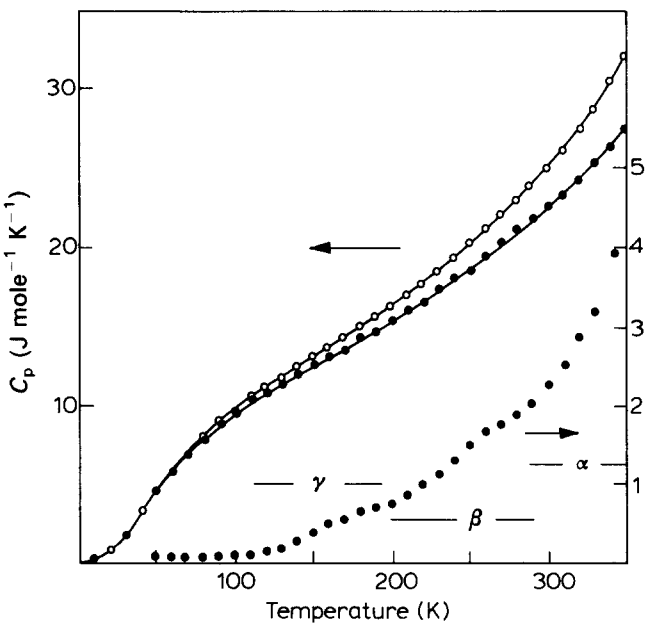

Figure 35 Heat capacity of LPE. Values for a 81% crystalline specimen (○) compared to extrapolated behaviour of 100% crystalline material; (●) (curves: left-hand ordinate scale). (Chang[93], Chang *et al.*[92]). A difference plot of these two curves is also shown (points only: right-hand ordinate scale). Approximate temperature ranges where mechanical relaxation occurs at low frequency (torsion pendulum) are indicated

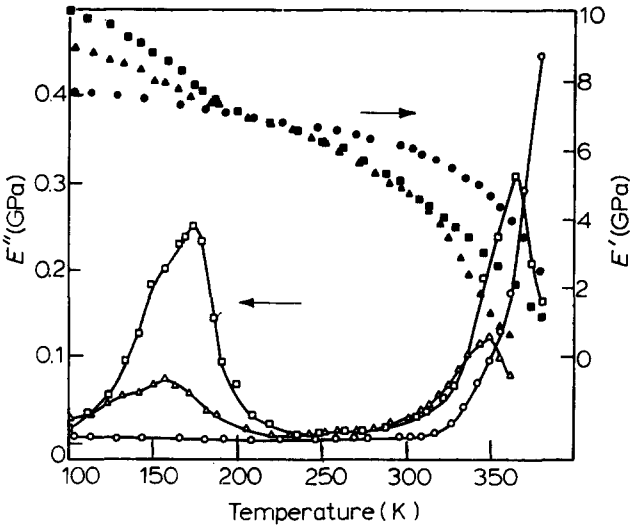

Figure 36 Complex tensile moduli of a paraffin ($C_{94}H_{190}$, (○), and (●)) and two low molecular weight LPE fractions ((△), and (▲) ≈1860 MW; squares, 3800 MW) compared (Crissmann[70])

interpreted as the glass–rubber relaxation of unconstrained amorphous PE. Above this temperature, crystallization ensued and a peak at 260 K was interpreted as the glass–rubber relaxation of the crystal-constrained amorphous fraction. A peak at 370 K was assigned as the α process. On performing recycles of the scan, a single broad β process centred at ≈230 K was observed between γ and α peaks. These findings are thus consistent with the relaxation behaviour of other crystalline polymers where crystallization and relaxation have been simultaneously studied.

The γ process

It was seen above that in lPE the γ mechanical relaxation correlates with crystallinity as an amorphous process. The same is true for the dielectric relaxation[56] and for the n.m.r. relaxation via broad-line proton resonance measurements (see *Figure 31*). Perhaps the most widely discussed aspect of γ process behaviour concerns the shapes of isochronal loss plots vs. temperature and their implication for phase assignment. That is, a low temperature tail and/or shoulder have often been interpreted as evidence for a complex process involving overlapping but distinct relaxations. Often the lower temperature portion has been supposed to be due to a contribution from the crystal phase. However it has already been seen that relaxation strength assessment now allows considerable confidence in assigning the process as completely amorphous phase in origin. It was remarked in the discussion of PET that broadening of the relaxation time distribution with decreasing temperature leads to the characteristic low temperature-side skewing of the subglass loss peak. The presence of a low temperature-side shoulder can be attributed to the freezing-in of the width of the distribution at low temperature. These same considerations hold true for lPE as well. Very good fits of the γ loss peak including the shoulder can be achieved (*Figure 25*) by invoking this kind of temperature dependence in the Cole–Cole $\bar{\alpha}$ parameter[29]. Just as for the β peak in PET (and the γ peak in aliphatic polyesters), the broadening of the γ process in the frequency domain with decreasing temperature can be demonstrated for lPE directly from isothermal dielectric measurements *versus* frequency[56].

Other evidence that the γ process in PE is of single phase origin can also be cited. The most rigorous way to exclude an amorphous fraction is to study a well-formed macroscopic single crystal. High molecular weight PE single crystals are of course microscopic and contain an amorphous layer comprising ≈20% of the material. However macroscopic single crystals of paraffins can be prepared. Crissman and Passaglia[69] found that very pure n-Eicosane (20 carbon atom paraffin) single crystals have no loss peaks at all. Later Crissman[70] showed that the very long chain paraffin n-$C_{94}H_{190}$, although polycyrstalline, shows no loss peaks (see *Figure 36*). A low molecular weight lPE fraction where the measured X-ray long period coincided with the chain length (indicating little or no chain folding as yet) but possessing measurable polydispersity (indicating the probability of a small amount of non-crystallized material) was also studied. This specimen showed the onset of both γ and α relaxations. A higher molecular weight fraction where the measured long period was now significantly less than the chain length (showing chain folding and hence an amorphous layer) now showed well developed γ and α processes. Other attempts have been made to eliminate the amorphous fraction. Nitric acid selectively attacks the amorphous material and in a n.m.r. study of single crystal mats treated this way it was found that the γ relaxation was nearly eliminated[72]. In an analogous mechanical study[100], a γ process was detected after nitric acid treatment. However the required encapsulation technique precluded quantitative assessment of the effect on relaxation strength. In general it is not really known how effective the treatment is in cleanly removing *all* the amorphous layer. Pressure has been used as a variable in attempting to resolve the γ process into possible components due to competing mechanisms. Processes with slightly different activation energies could be expected to have somewhat different pressure coefficients of isochronal T_{max} with the higher activation energy, higher T_{max} component likely to have the higher coefficient. Hence the components would become better resolved at higher pressure. However, as may be seen in *Figure 37*, dielectric loss results[101] on lightly oxidized lPE show no evidence for resolution into separate processes at pressures up to >4 kbar. Another experiment that can in principle help distinguish crystalline and amorphous phase contributions is measurement of relaxation anisotropy[61]. In *Figure 28* for lPE and bPE it may be seen that the anisotropy in the γ process is much less than for the α (the latter arising of course in the crystals). The level of γ relaxation anisotropy is consistent with some amorphous phase orientation being induced by the crystal orientation. Especially important is the observation that there is no difference in shape of the curves in the two directions as would be expected if contributions from two components were being selectively monitored. The degree of crystallinity does not have a strong influence on the relaxation behaviour (beyond the strength) (see *Figure 20* and *Figure 37*) but some slight trends are noticeable. There is some tendency for the γ process to become broader as crystallinity increases. The loss location as measured mechanically (isochronal T_{max}) moves to higher temperature with crystallinity (*Figure 20*) but no trend was found dielectrically[56]. In any event the changes observed are not of the kind to be attributed to varying relative contributions from distinct processes but rather

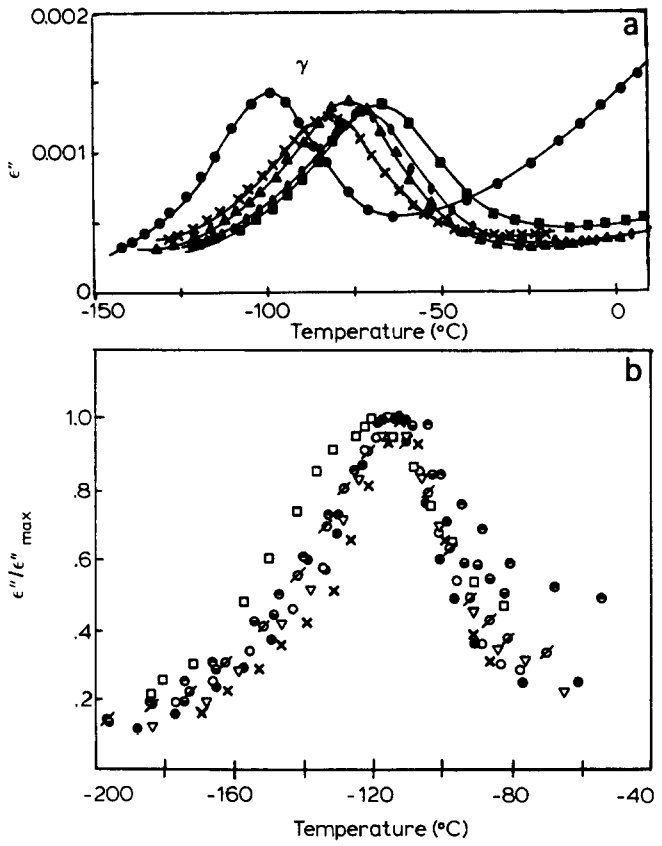

Figure 37 The shape of the γ process in LPE (dielectric results). (a) The effect of pressure ((●), 1 atm.; (×), 2.13; (▲), 2.80; (●), 3.50; (■), 4.19 kBar; isochronal scans at 1 kHz; (Sayre *et al.*[101]). (b) The effect of crystallinity ((×), 938; (●), 959; (○), 961; (◐), 963; (△), 968; (○), 972; (◑), 992 kg/m^3; (□), BPE; 10Hz Ashcraft and Boyd[56])

to the effect of crystallinity on the parameters of a single broad process. It was noted above (*Figure 33*) that the γ process in completely amorphous partially chlorinated bPE is similar to that in other PE's. The evidence is thus very strong that the γ process in PE arises as a single process in the amorphous phase. As already mentioned there is less evidence for other polymers. As was discussed above, the behaviour of iPP is consistent with this assignment also. The γ relaxation in polytetrafluoroethylene has been shown to extrapolate cleanly vs. crystallinity as an amorphous process[4,102]. Although only two crystallinities are shown it is evident in *Figure 22* that for POM both the relaxation strength and tan δ point to amorphous origin for the γ relaxation.

Newer n.m.r. techniques show promise of giving more detail as to the kinds of molecular motion underlining subglass transitions like the γ relaxation in PE. Sillescu, Spiess and coworkers[103-105] have studied the deuterium quadrupole resonance in lPE with interesting conclusions. This technique has the advantage of being insensitive to long-range interactions and being responsive to reorientations of the C–D vector. The fundamental line shapes are known and analysis of experimental line shapes in terms of models is fairly direct[104]. The Pake spectrum for deuterons in a rigid solid found at low temperature changed with increasing temperature. The spectrum in the temperature–frequency region of the γ relaxation could be interpreted as a superposition of the rigid spectrum and one corresponding to C–D bond reorientation through the tetrahedral angles allowed by a local three-bond crankshaft-like motion. At higher temperatures, corresponding to the β relaxation region, it was found that a model with longer range reorientations was necessary to account for the narrow centre component appearing in the spectrum. However even at the higher temperatures the model appropriate to the spectrum incorporated considerable constraint on configurational reorientation. This of course is in accord with conclusions from other measurements.

Relaxation in semicrystalline polymers cannot be discussed without commenting on the behaviour of polychlorotrifluoroethylene (PCTFE). The paper of Hoffman, Williams and Passaglia[106] deservedly has had more influence on the interpretation of relaxation processes in crystalline polymers than any other publication. Although their work dealt in detail with mechanistic models for PE they drew heavily from the experimental side from their own dielectric studies on PCTFE[107] and from McCrum's mechanical measurements[108] on the same material. In broad outline their mechanistic conclusions have turned out to be remarkably correct. However PCTFE in many respects is atypical in its behaviour and its peculiarities need to be discussed. The principal way in which it differs from lPE is in the phase assignment of the γ relaxation. A great detal of evidence has been presented

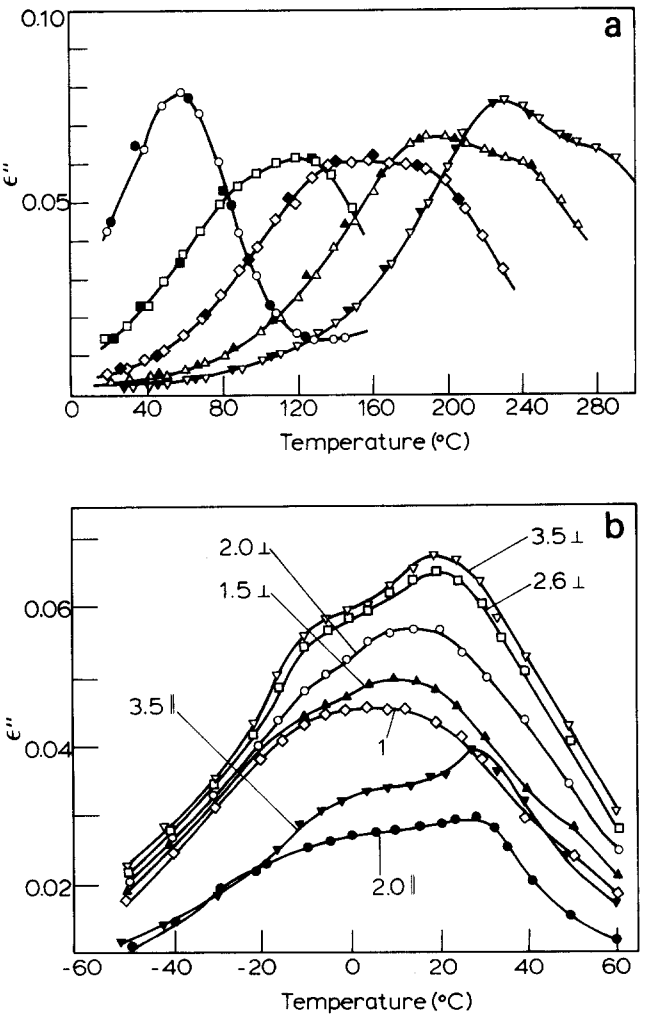

Figure 38 The shape of the γ process in PCTFE (dielectric results). (a) The effect of pressure ((○) 1 atm.; (□), 5; (◇), 10; (△), 15; (▽), 20 kBar); isochronal scans at 10 kHz; Samara and Fritz[109]). (b) The effect of orientation (draw ratios and directions measured are indicated; Choy *et al.*[110])

above that in lPE only the amorphous phase is involved. This appears not to be true for PCTFE and many of the same criteria used for judging phase assignment for the γ process in lPE lead to the conclusion that PCTFE has a partial crystalline origin. This chance happening no doubt was instrumental in motivating HWP to stress the possibility of partial crystalline origin in lPE. The mechanical measurements[108] comprised only three specimens and no firm conclusion with respect to phase origin can be made. However from the variation of dielectric relaxation strength with crystallinity it is difficult to escape the conclusion that the γ process is present also in the crystal fraction. Two other experiments, of types discussed above, the effect of pressure[109] and orientation[110] on relaxation, also indicate two phase origin (see *Figure 38*). It is important of course to understand why this polymer should differ from PE and a number of other crystalline polymers in the phase assignment of the low temperature relaxation. The reason probably lies in the crystal structure. The polymer repeat unit contains an asymmetric centre and the question of tactic perfection arises. This seems to translate into a highly imperfect chain packing that resembles that of a liquid crystal[111]. This disordered packing would be much more tolerant of conformational reorientation than a well ordered structure. It is doubtful that polymers with well-developed three dimensional unit cells could show a crystalline contribution to a γ process.

Much of the experimental behaviour detailed in the present article can be rationalized at least qualitatively in terms of molecular processes. Some of it can be described in fair detail via molecular models or theories. Some of it shows the inadequacy of present models. The molecular interpretation will be reviewed in a separate article.

ACKNOWLEDGEMENT

The author is grateful to the National Science Foundation, Division of Materials Research, Polymers Program, for support of his research on relaxations in general and the preparation of this article in particular.

REFERENCES

1 McCrum, N. G., Read, B. E. and Williams, G. 'Anelasitic and Dielectric Effects in Polymeric Solids', Wiley, New York, NY, 1967
2 Manson, J. A. and Sperling, L. H. 'Polymer Blends and Composites', Plenum, New York, 1976
3 Nielsen, L. E. *J. Appl. Polym. Sci.* 1975, **19**, 1485
4 Gray, R. W. and McCrum, N. G. *J. Polym. Sci. Part A-2* 1969, **8**, 1329
5 Halpin, J. C. and Kardos, J. L. *J. Appl. Phys.* 1972, **43**, 2235
6 Kardos, J. L. and Raisoni, J. *Polym. Eng. Sci.* 1975, **15**, 183
7 Wang, T. T. *J. Appl. Phys.* 1973, **44**, 2218
8 Wang, T. T. *J. Appl. Phys.* 1973, **44**, 4052
9 Wang, T. T. *J. Polym. Sci. Polym. Phys. Edn.* 1974, **12**, 145
10 McCullough, R. L. in 'Treatise on Materials Science and Technology', Vol. 10-B, (Ed. J. M. Schultz), Academic Press, New York (1977)
11 Hashin, Z. and Shtrikman, J. *J. Mech. Physl. Solids* 1963, **11**, 127
12 Halpin, J. C. and Kardos, J. L. *Polym. Eng. Sci.* 1976, **16**, 344
13 Boyd, R. H. *Polym. Eng. Sci.* 1979, **14**, 1010
14 Hill, R. *J. Mech. Phys. Solids* 1964, **12**, 199
15 Hermans, J. J. *Proc. K. Ned. Akad. Wet.* 1967, **B70**, 1
16 Boyd, R. H. *J. Polym. Sci. Polym. Phys. Edn.* 1983, **21**, 493
17 Hashin, Z. and Shtrikman, S. *J. Appl. Phys.* 1962, **33**, 3125
18 Boyd, R. H. *J. Polym. Sci. Polym. Phys. Edn.* 1983, **21**, 505
19 Illers, K. H. and Breuer, H. *J. Colloid Sci.* 1963, **18**, 1
20 Kilian, H. G., Halboth, H. and Jenckel, E. *Kolloid Z.* 1960, **172**, 166
21 Ishida, Y., Yamafuji, K., Ito, H. and Takayanagi, M. *Koll. Z. Z. Polym.* 1962, **184**, 97
22 Saito, S. *Koll. Z. Z. Polym.* 1963, **189**, 116
23 Coburn, J. C. and Boyd, R. H. Ph.D. Dissertation, (Coburn), U. Utah, to be published 1984
24 Havriliak, S. and Negami, S. *Polymer* 1967, **8**, 161
25 Yoshihara, M. and Work, R. N. *J. Chem. Phys.* 1980, **72**, 5909
26 Cole, K. S. and Cole, R. H. *J. Chem. Phys.* 1941, **9**, 341
27 Davidson, D. W. and Cole, R. H. *J. Chem. Phys.* 1950, **18**, 1417
28 Ishida, Y., Matsuo, M. and Yamafuji, K. *Kolloid Z.* 1962, **180**, 108
29 Boyd, R. H. *Macromol.* 1984, **7**, 903
30 Boyd, R. H. 1984, unpublished results
31 Wall, R. A., Sauer, J. A. and Woodward, A. E. *J. Polym. Sci.* 1959, **35**, 281
32 Newman, S. and Cox, W. P. *J. Polym. Sci.* 1960, **46**, 29
33 Fuoss, R. M. *J. Am. Chem. Soc.* 1941, **63**, 369
34 Ishida, Y. *Kolloid Z.* 1960, **168**, 29
35 Soni, P. L., Geil, P. H. and Collins, E. A. *J. Macromol. Sci.-Phys.* 1981, **B20**, 479
36 Boyd, R. H. and Porter, C. H. *J. Polym. Sci. A-2* 1972, **10**, 647
37 Boyd, R. H. *J. Chem. Phys.* 1959, **30**, 1276
38 Woodward, A. E., Crissman, J. M. and Sauer, J. A. *J. Polym. Sci.* 1960, **44**, 23
39 Ito, M., Nakatani, S., Gokan, A. and Tanaka, K. *J. Polym. Sci. Polym. Phys. Edn.* 1977, **15**, 605
40 Ito, M., Kubo, M., Tsuruta, A. and Tanaka, K. *J. Polym. Sci. Polym. Phys. Edn.* 1978, **16**, 1435
41 Pochan, J. M. and Hinman, D. F. *J. Polym. Sci. Polym. Phys. Edn.* 1975, **13**, 1365
42 Aylwin, P. A. and Boyd, R. H. *Polymer* 1984, **25**, 323
43 Boyd, R. H. and Aylwin, P. A. *Polymer* 1984, **25**, 330
44 Boyd, R. H. and Aylwin, P. A. *Polymer* 1984, **25**, 340
45 Boyd, R. H. and Hasan, A. A. *Polymer* 1984, **25**, 347
46 Illers, K. H. *Koll. Z. Z. Polym.* 1969, **231**, 622
47 Stehling, F. C. and Mandelkern, L. *Macromol.* 1970, **3**, 242
48 Pechhold, W., Eisele, U. and Knauss, G. *Koll. Z. Z. Polym.* 1964, **196**, 27
49 Crissman, J. M. and Passaglia, E. *J. Res. Natl. Bur. Stand.* 1966, **70A**, 225
50 Cooper, J. W. and McCrum, N. G. in 'Adv. in Polym. Sci. and Eng.' (Eds. K. D. Pae, D. R. Morrow and Y. Chen), Plenum Press, New York (1972)
51 Illers, K. H. *Koll. Z. Z. Polym.* 1973, **251**, 394
52 Passaglia, E. and Martin, G. M. *J. Res. Natl. Bur. Stand.* 1964, **68**, 519
53 McCrum, N. G. *J. Polym. Sci.* 1961, **54**, 561
54 Eby, R. K. *J. Acoust. Soc. Sm.* 1964, **36**, 1485
55 Boyd, R. H. and Biliyar, K. *Am. Chem. Soc. Div. Polym. Chem. Polym. Prepr.* 1973, **14**, 329
56 Ashcraft, C. R. and Boyd, R. H. *J. Polym. Sci. Polym. Phys. Edn.* 1976, **14**, 2153
57 Buckley, C. P. and McCrum, N. G. *J. Mater. Sci.* 1973, **8**, 928
58 Davies, G. R., Owen, A. J., Ward, I. M. and Gupta, V. B. *J. Macromol. Sci.-Phys.* 1976, **B6**, 215
59 Zannetti, R., Fichera, A., Celotti, G. and Ferrero Martelli, A. *Eur. Polym. J.* 1968, **4**, 399
60 Flocke, H. A. *Kolloid Z.* 1962, **180**, 118
61 Boyd, R. H. and Yemni, T. *Polym. Eng. Sci.* 1979, **14**, 1023
62 Nakayasu, H., Markovitz, H. and Plazek, D. J. *Trans. Soc. Rheol.* 1961, **5**, 261
63 McCrum, N. G. and Morris, E. L. *Proc. Roy. Soc. (London)* 1966, **A292**, 506
64 Sinnott, K. M. *J. Appl. Phys.* 1966, **37**, 3385
65 Takayanagi, M. *Pure Appl. Chem.* 1967, **15**, 555
66 Manabe, S., Sakoda, A., Katada, A. and Takayanagi, M. *J. Macromol. Sci.-Phys.* 1970, **B4**, 161
67 Kajiyama, T., Okada, T., Sakoda, A. and Takayanagi, M. *J. Macromol. Sci.-Phys.* 1973, **B7**, 583
68 Meakins, R. J. *Progr. Dielectr.* 1961, **3**, 153
69 Crissman, J. M. and Passaglia, E. *J. Appl. Phys.* 1971, **42**, 4636
70 Crissman, J. M. *J. Polym. Sci. Polym. Phys. Edn.* 1975, **13**, 1407
71 Olf, H. G. and Peterlin, A. *J. Polym. Sci. A-2* 1970, **8**, 753
72 Olf, H. G. and Peterlin, A. *J. Polym. Sci. A-2* 1970, **8**, 771
73 McBrierty, V. J. and McDonald, I. R. *Polymer* 1975, **16**, 125
74 Opella, S. J. and Waugh, J. S. *J. Chem. Phys.* 1977, **66**, 4919
75 Olf, H. G. and Peterlin, A. *J. Polym. Sci. A-2* 1970, **8**, 791
76 Gray, R. W. *J. Mater. Sci.* 1973, **8**, 1673

77 McCrum, N. G. *J. Mater. Sci.* 1978, **13**, 1596
78 McBrierty, V. J. *Polymer* 1974, **15**, 503
79 McCall, D. W. *Natl. Bur. Stand. Spec. Publ.* 1969, **310**, 475
80 Bergmann, K. *Koll. Z. Z. Polym.* 1973, **251**, 962
81 Bergmann, K. *J. Polym. Sci. Polym. Phys. Edn.* 1978, **16**, 1611
82 Illers, K. H. *Koll. Z. Z. Polym.* 1972, **250**, 426
83 Arai, H. and Kuriyama, I. *Coll. Polym. Sci.* 1976, **254**, 967
84 Schmieder, K. and Wolf, K. *Koll. Z.* 1953, **134**, 149
85 Nielsen, L. E. *J. Polym. Sci.* 1960, **42**, 357
86 Earnest, T. R. and MacKnight, W. J. *Macromolecules* 1977, **10**, 206
87 Reding, F. P., Faucher, J. A. and Whitman, R. D. *J. Polym. Sci.* 1962, **57**, 483
88 Phillips, P. J., Emerson, F. A. and MacKnight, W. J. *Macromolecules* 1970, **3**, 767
89 Otocka, E. P. and Kwei, T. K. *Macromolecules* 1968, **1**, 244
90 Wilson, T. P., Von Dohlen, W. C. and Koleske, J. V. *J. Polym. Sci. Polym. Phys. Edn.* 1974, **12**, 1607
91 Popli, R. and Mandelkern, L. *Polym. Bull.* 1983, **9**, 260
92 Chang, S. S., Westrum, E. F., Jr. and Carlson, H. G. *J. Res. Natl. Bur. Stand.* 1975, **79A**, 437
93 Chang, S. S. *J. Res. Natl. Bur. Stand.* 1974, **78A**, 387
94 Gaur, U. and Wunderlich, B. *J. Chem. Phys. Ref. Data* 1981, **10**, 119
95 Beatty, C. L. and Karasz, F. E. *J. Macromol. Sci.-Rev. Macromol. Chem.* 1979, **C17**, 37
96 Davis, G. T. and Eby, R. K. *J. Appl. Phys.* 1973, **44**, 4274
97 Boyer, R. F. *Macromolecules* 1973, **6**, 288
98 Lam, R. and Geil, P. H. *Polym. Bull.* 1978, **1**, 127
99 Lam, R. and Geil, P. H. *J. Macromol. Sci.-Phys.* 1981, **B20**, 37
100 Shen, M. and Cirlin, E. H. *J. Macromol. Sci.-Phys.* 1970, **B4**, 947
101 Sayre, J. A., Swanson, S. R. and Boyd, R. H. *J. Polym. Sci. Polym. Phys. Edn.* 1978, **16**, 1739
102 McCrum, N. G. in 'Molecular Basis of Transitions and Relaxations', (Ed. D. J. Meier), Midland Macromol. Inst., Mono No. 4 (1978)
103 Hentschel, D., Sillescu, H. and Spiess, H. W. *Macromolecules* 1981, **14**, 1605
104 Rosenke, K., Sillescu, H. and Spiess, H. W. *Polymer* 1980, **21**, 757
105 Spiess, H. W. *Coll. Polym. Sci.* 1983, **261**, 193
106 Hoffman, J. D., Williams, G. and Passaglia, G. *J. Polym. Sci. Part C* 1966, **14**, 173
107 Scott, A. H., Scheiber, D. J., Curtis, A. J., Lauritzen, J. I. and Hoffman, J. D. *J. Res. Natl. Bur. Stand.* 1962, **66A**, 269
108 McCrum, N. G. *J. Polym. Sci.* 1959, **34**, 355
109 Samara, G. A. and Fritz, I. J. *J. Polym. Sci. Polym. Lett. Edn.* 1975, **13**, 93
110 Choy, C. L., Cheng, K. H. and Hsu, B. S. *J. Polym. Sci. Polym. Phys. Edn.* 1981, **19**, 991
111 Khoury, F. and Passaglia, E. in 'Treatise on Solid State Chemistry', Vol. 3, (Ed. N. B. Hannay), Plenum Press, New York (1976)
112 Popli, R., Glotin, M., Mandelkern, L. and Benson, R. S. *J. Polym. Sci. Polym. Phys. Edn.* 1984, **22**, 407